GAMMA-RAY STRENGTH-FUNCTION MEASUREMENTS AT ELBE

R. Schwengner[1], G. Rusev[1,2], N. Tsoneva[3], N. Benouaret[1,4], R. Beyer[1], F. Dönau[1], M. Erhard[1], S. Frauendorf[1,5], E. Grosse[1,6], A. R. Junghans[1], J. Klug[1], K. Kosev[1], H. Lenske[3], C. Nair[1], K. D. Schilling[1], A. Wagner[1]

[1] *Institut für Strahlenphysik, Forschungszentrum Dresden-Rossendorf, 01314 Dresden, Germany*
[2] *Dept. of Physics, Duke University and Triangle Universities Nuclear Laboratory, Durham, NC 27708*
[3] *Institut für Theoretische Physik, Universität Gießen, 35392 Gießen, Germany*
[4] *Faculté de Physique, Université des Sciences et de la Technologie d'Alger, 16111 Bab-Ezzouar, Algerie*
[5] *Department of Physics, University of Notre Dame, Notre Dame, IN 46556*
[6] *Institut für Kern- und Teilchenphysik, Technische Universität Dresden, 01062 Dresden, Germany*

- The bremsstrahlung facility
- Photon-scattering experiments
- Data analysis and results
- QRPA and QPM calculations
- Photoactivation experiments

Supported by Deutsche Forschungsgemeinschaft

Dipole strength close to the particle-separation energy

- Understanding of astrophysical processes:
  - Influence on (γ,n) reaction rates in the p-process.
  - Influence on (n,γ) reaction rates in the s-process.
- Studies for transmutation:
  - Analysis of (n,γ) reactions.
- Open problems:
  - Precise knowledge of the $E1$ strength on the low-energy tail of the Giant Dipole Resonance.
  - Properties of the $E1$ strength functions at varying proton and neutron numbers: shell effects, deformation etc.

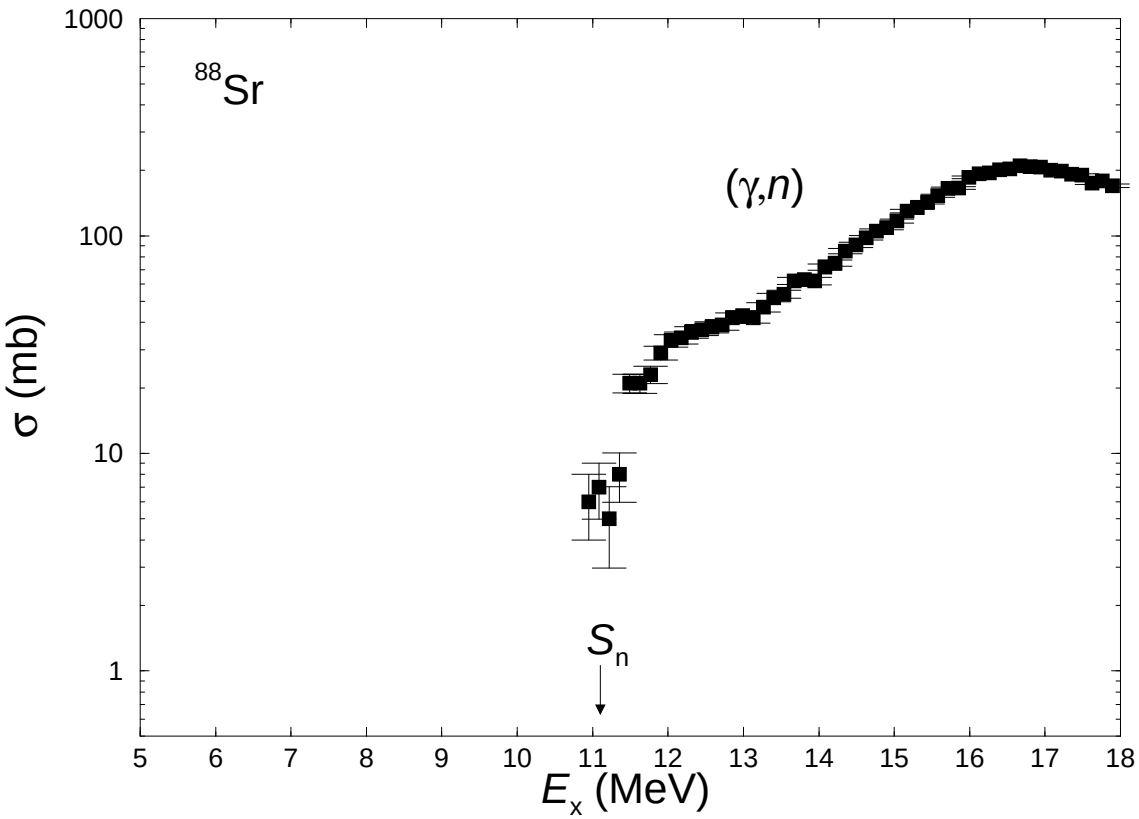

Dipole strength close to the particle-separation energy

- Understanding of astrophysical processes:
  - Influence on (γ,n) reaction rates in the p-process.
  - Influence on (n,γ) reaction rates in the s-process.
- Studies for transmutation:
  - Analysis of (n,γ) reactions.
- Open problems:
  - Precise knowledge of the $E1$ strength on the low-energy tail of the Giant Dipole Resonance.
  - Properties of the $E1$ strength functions at varying proton and neutron numbers: shell effects, deformation etc.

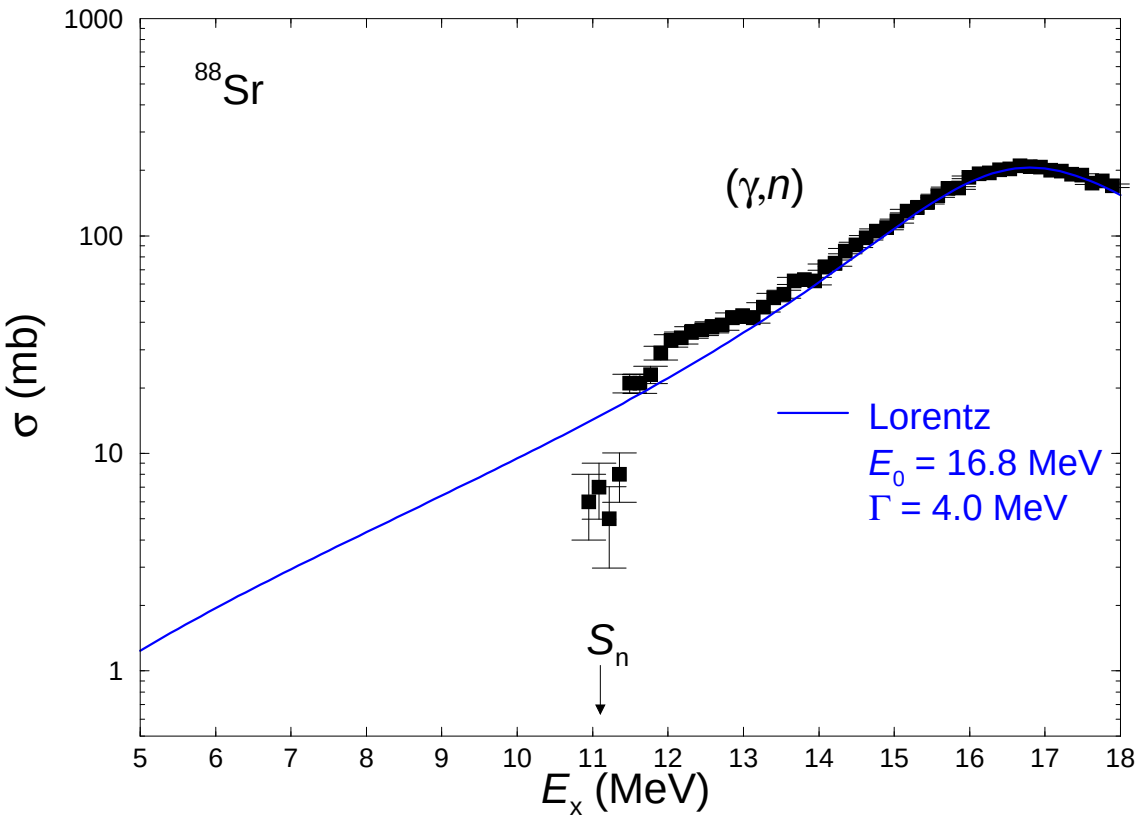

Dipole strength close to the particle-separation energy

- Understanding of astrophysical processes:
  - Influence on (γ,n) reaction rates in the p-process.
  - Influence on (n,γ) reaction rates in the s-process.
- Studies for transmutation:
  - Analysis of (n,γ) reactions.
- Open problems:
  - Precise knowledge of the $E1$ strength on the low-energy tail of the Giant Dipole Resonance.
  - Properties of the $E1$ strength functions at varying proton and neutron numbers: shell effects, deformation etc.

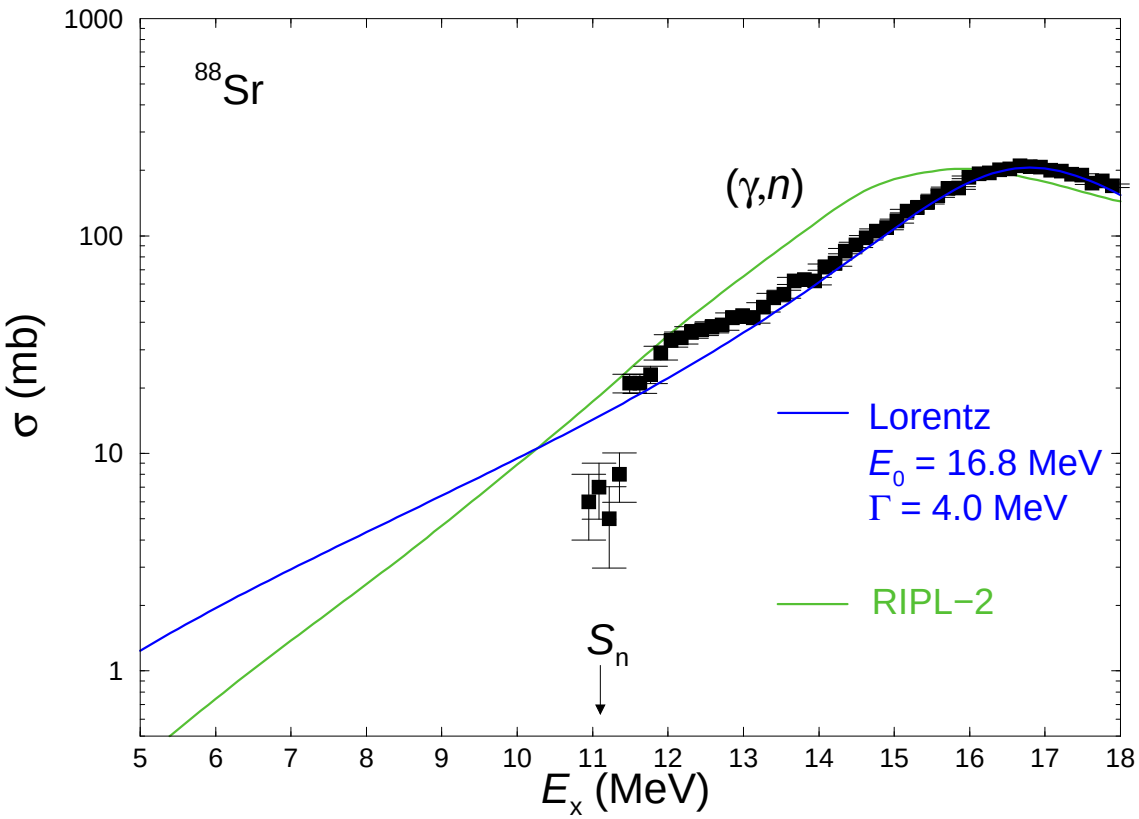

Dipole strength close to the particle-separation energy

- Understanding of astrophysical processes:
  - Influence on (γ,n) reaction rates in the p-process.
  - Influence on (n,γ) reaction rates in the s-process.
- Studies for transmutation:
  - Analysis of (n,γ) reactions.
- Open problems:
  - Precise knowledge of the $E1$ strength on the low-energy tail of the Giant Dipole Resonance.
  - Properties of the $E1$ strength functions at varying proton and neutron numbers: shell effects, deformation etc.

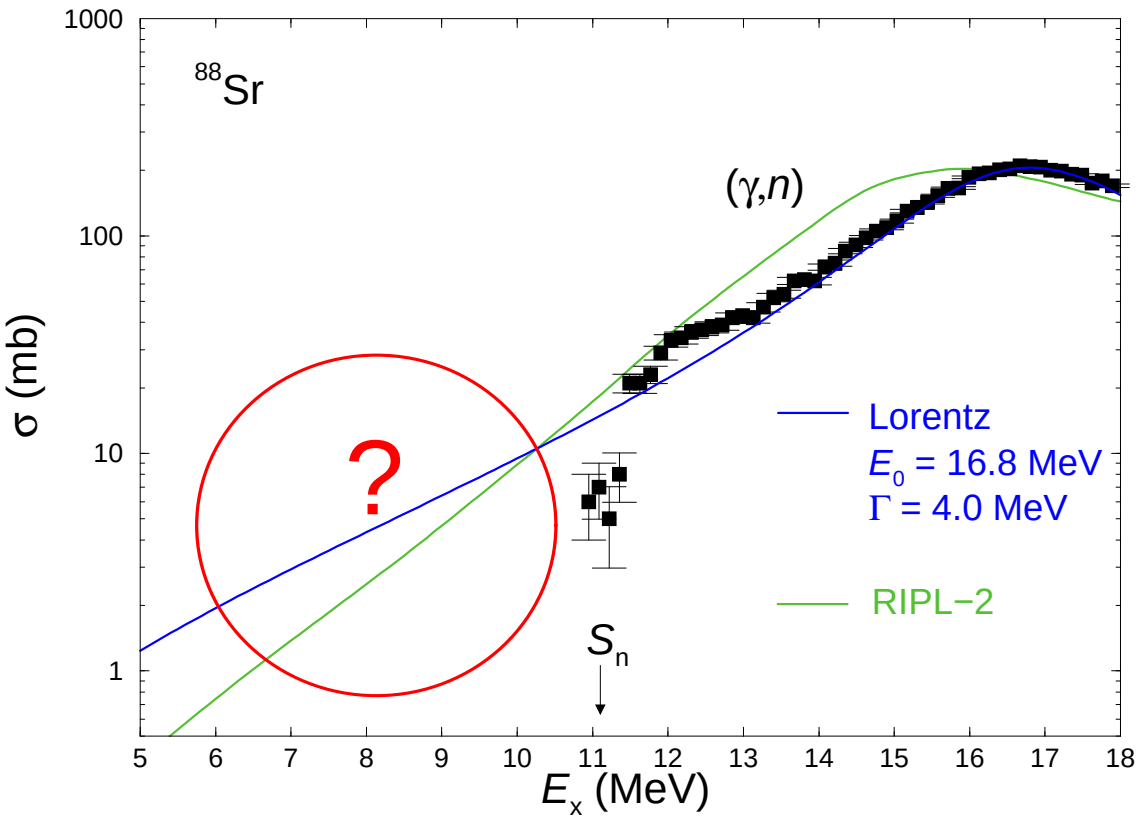

Electron Linear accelerator of high Brilliance and low Emittance

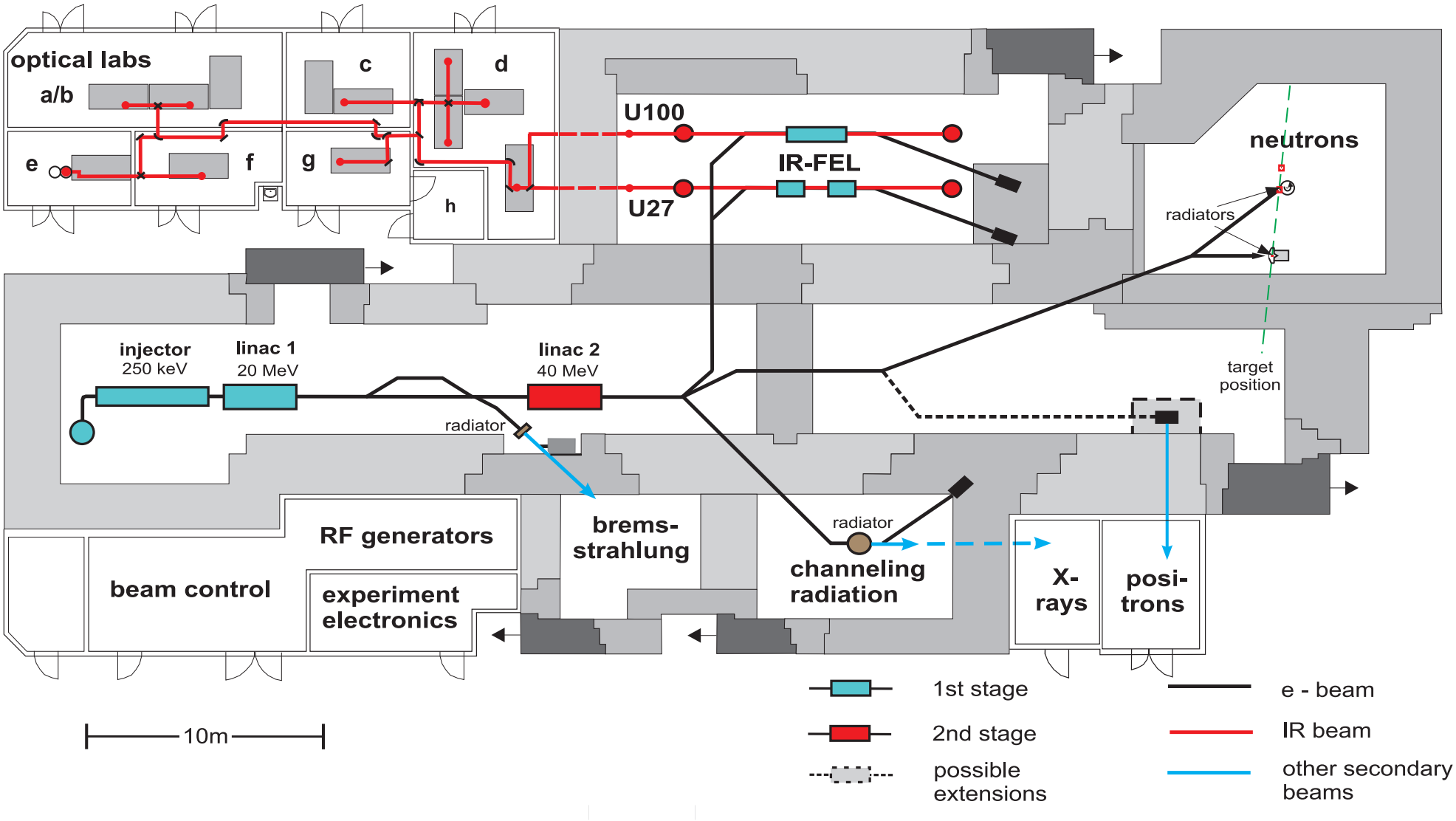

The bremsstrahlung facility at the electron accelerator ELBE

R.S. et al., NIM A 555 (2005) 211

Accelerator parameters:

- Maximum electron energy:
  18 MeV
- Maximum average current:
  1 mA
- Micro-pulse rate:
  13 MHz
- Micro-pulse length:
  $\approx$ 5 ps

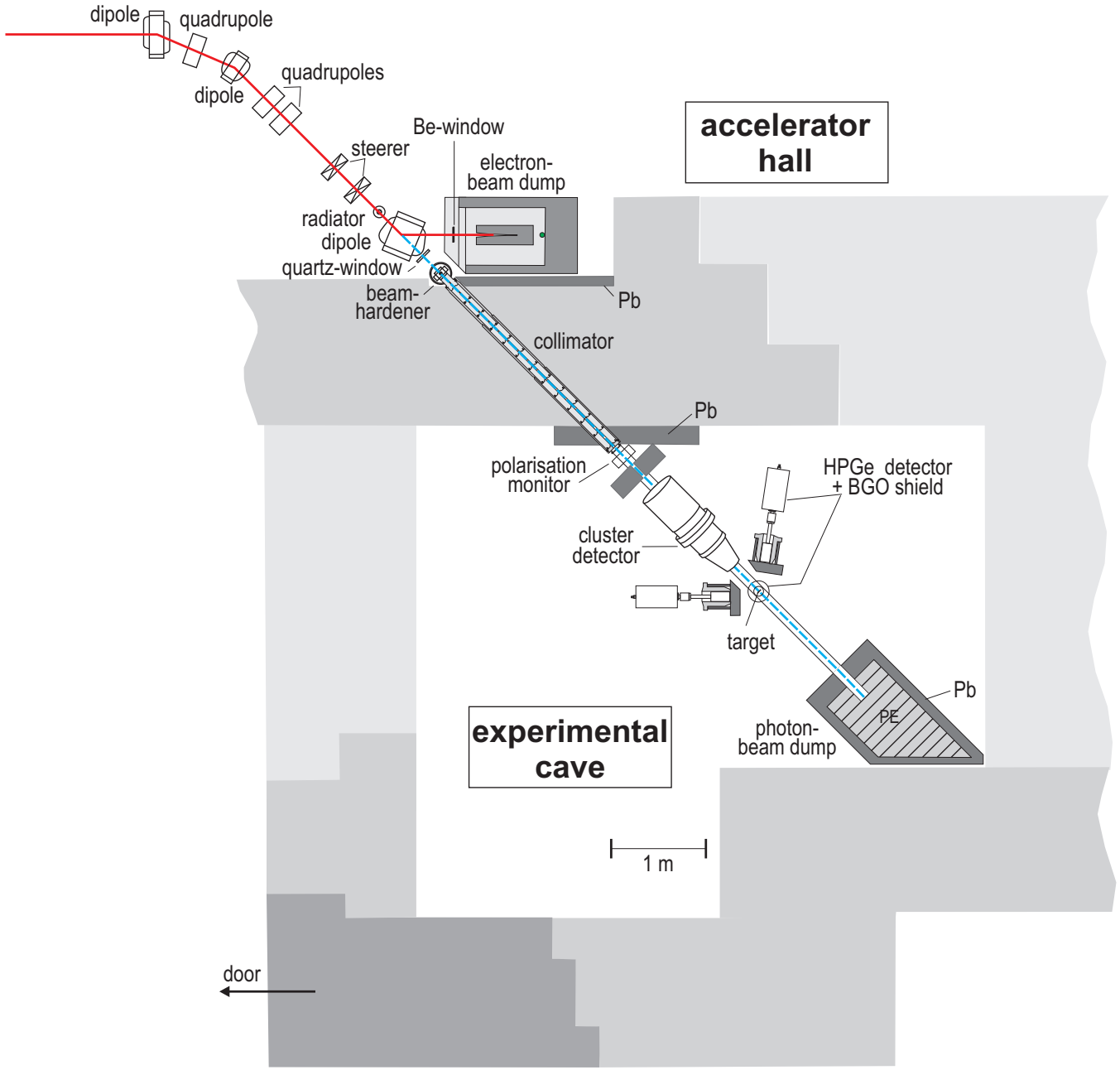

Detector setup

Nuclides under investigation in photon-scattering experiments

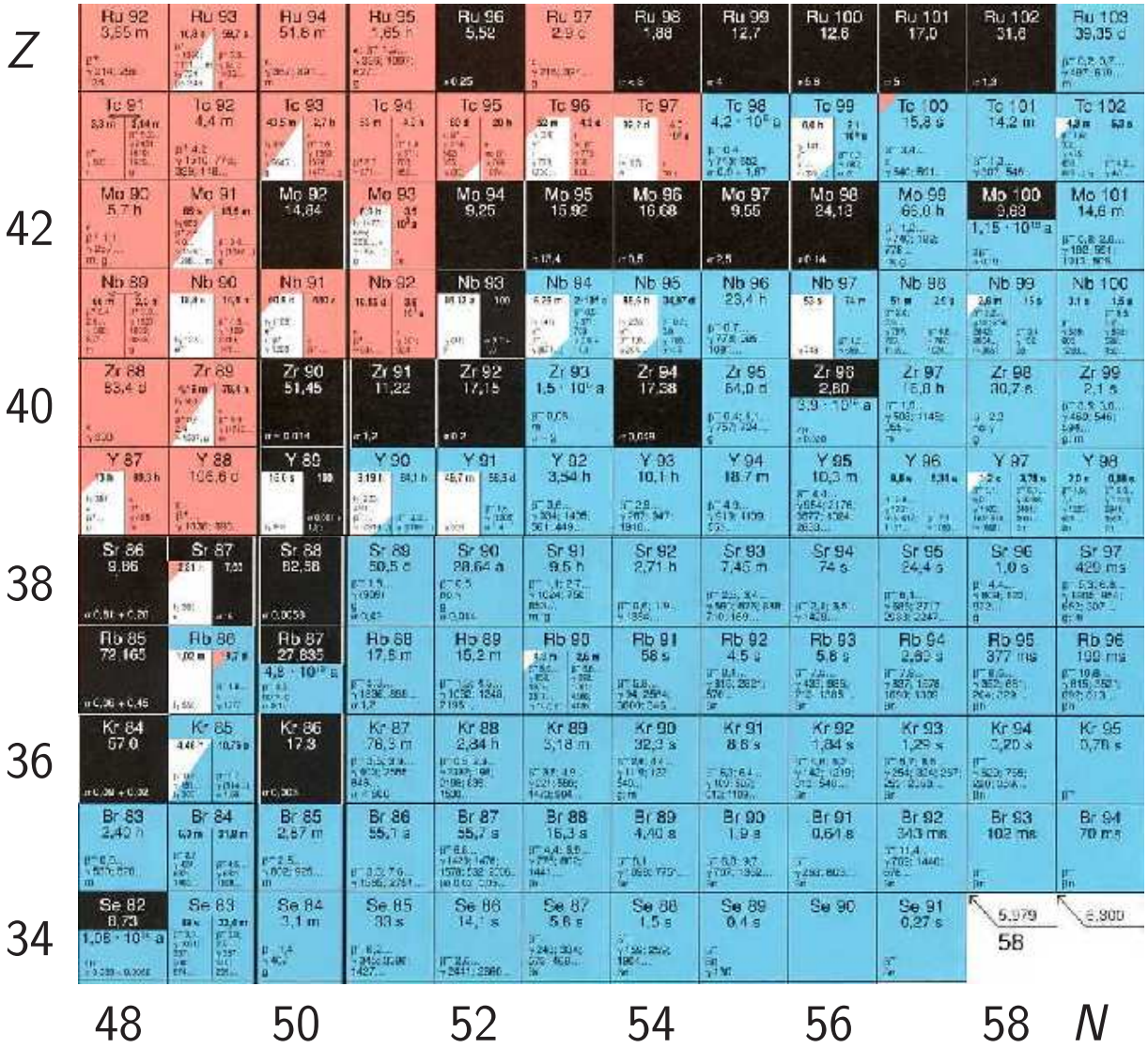

nuclide	S_n MeV	E_e^{kin} (MeV) ELBE
^{92}Mo	12.7	6.0[a], 13.2[b,c,d]
^{94}Mo	9.7	13.2[d]
^{96}Mo	9.2	13.2[d]
^{98}Mo	8.6	(3.3, 3.8)[a,e], (8.5, 13.2)[b,c,d]
^{100}Mo	8.3	(3.2, 3.4, 3.8)[a], (7.8, 13.2)[b,c,d]
^{90}Zr	12.0	7.0, 9.0, 13.2
^{89}Y	11.5	7.0[f], 9.5, 13.2
^{88}Sr	11.1	6.8[g], (9.0, 13.2, 16.0)[h]
^{87}Rb	9.9	4.0[i], 13.2
^{86}Kr	9.9	11.5

[a] G. Rusev et al., PRC 73 (2006) 044308
[b] R. Schwengner et al., NPA 788 (2007) 331c
[c] G. Rusev et al., PRC 77 (2008) 064321
[d] A. Wagner et al., JPG 35 (2008) 014035
[e] G. Rusev et al., PRL 95 (2005) 062501
[f] J. Reif et al., NPA 620 (1997) 1
[g] L. Käubler et al., PRC 70 (2004) 064307
[h] R. Schwengner et al., PRC 76 (2007) 034321
[i] L. Käubler et al., PRC 65 (2002) 054315

Problem of feeding and branching

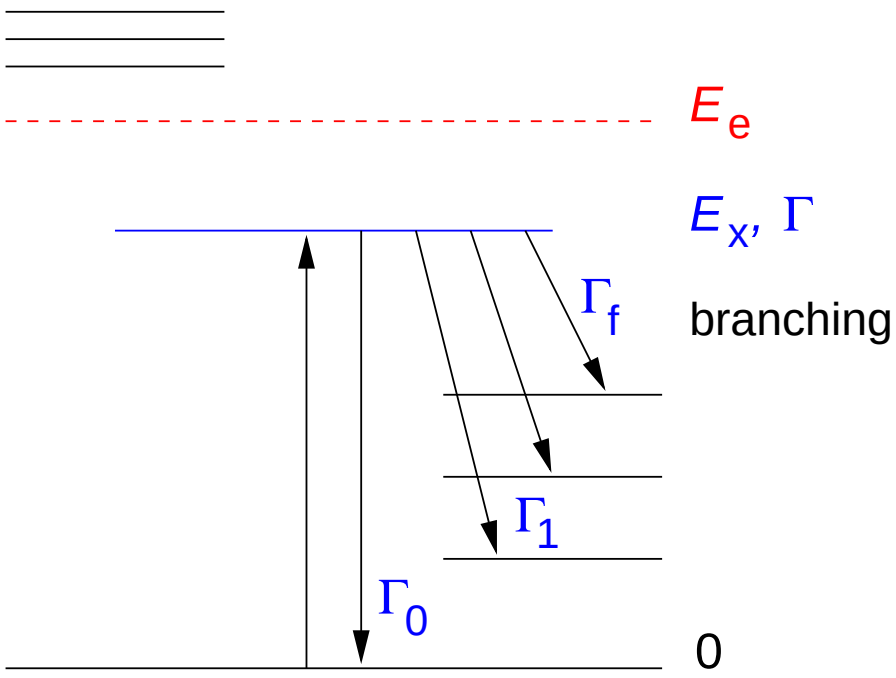

Measured intensity of a γ transition:

$$I_\gamma(E_\gamma, \Theta) = I_s(E_x)\, \Phi_\gamma(E_x)\, \epsilon(E_\gamma)\, N_{at}\, W(\Theta)\, \Delta\Omega$$

Scattering cross section integral:

$$I_s = \int \sigma_{\gamma\gamma}\, dE = \frac{2J_x + 1}{2J_0 + 1} \left(\frac{\pi\hbar c}{E_x}\right)^2 \frac{\Gamma_0}{\Gamma}\, \Gamma_0$$

Absorption cross section:

$$\sigma_\gamma = \sigma_{\gamma\gamma} \left(\frac{\Gamma_0}{\Gamma}\right)^{-1}$$

E1 strength:

$$B(E1) \sim \Gamma_0 / E_\gamma^3$$

Problem of feeding and branching

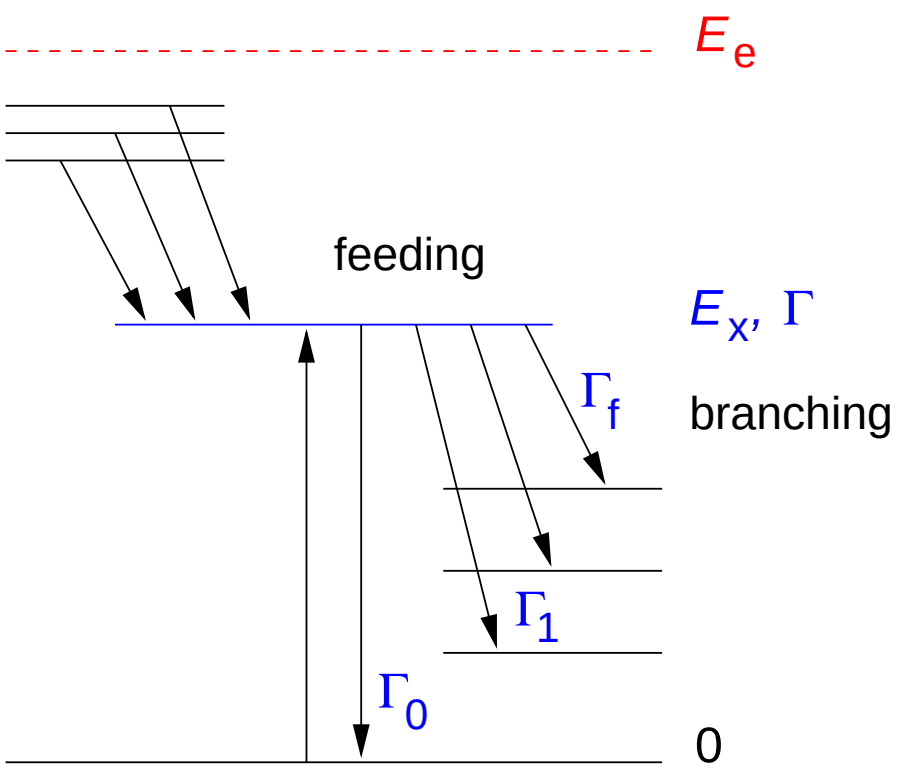

Measured intensity of a γ transition:

$$I_\gamma(E_\gamma, \Theta) > I_s(E_x)\, \Phi_\gamma(E_x)\, \epsilon(E_\gamma)\, N_{at}\, W(\Theta)\, \Delta\Omega$$

Scattering cross section integral:

$$I_s = \int \sigma_{\gamma\gamma}\, dE = \frac{2J_x + 1}{2J_0 + 1} \left(\frac{\pi\hbar c}{E_x}\right)^2 \frac{\Gamma_0}{\Gamma}\, \Gamma_0$$

Absorption cross section:

$$\sigma_\gamma = \sigma_{\gamma\gamma} \left(\frac{\Gamma_0}{\Gamma}\right)^{-1}$$

E1 strength:

$$B(E1) \sim \Gamma_0 / E_\gamma^3$$

Absolute detector efficiency and photon flux

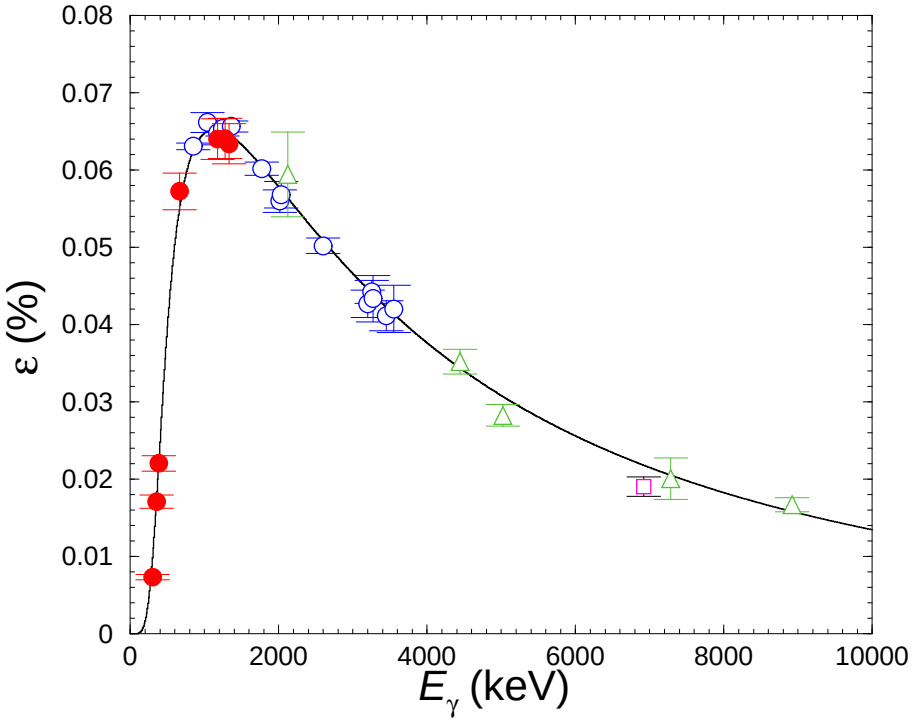

Absolute efficiency of two detectors at 127° deduced from ^{22}Na, ^{60}Co, ^{133}Ba, (filled circles) and simulated with GEANT3 (solid line). Relative efficiencies deduced from ^{56}Co (open circles), ^{11}B (open triangles) and ^{16}O (open square).

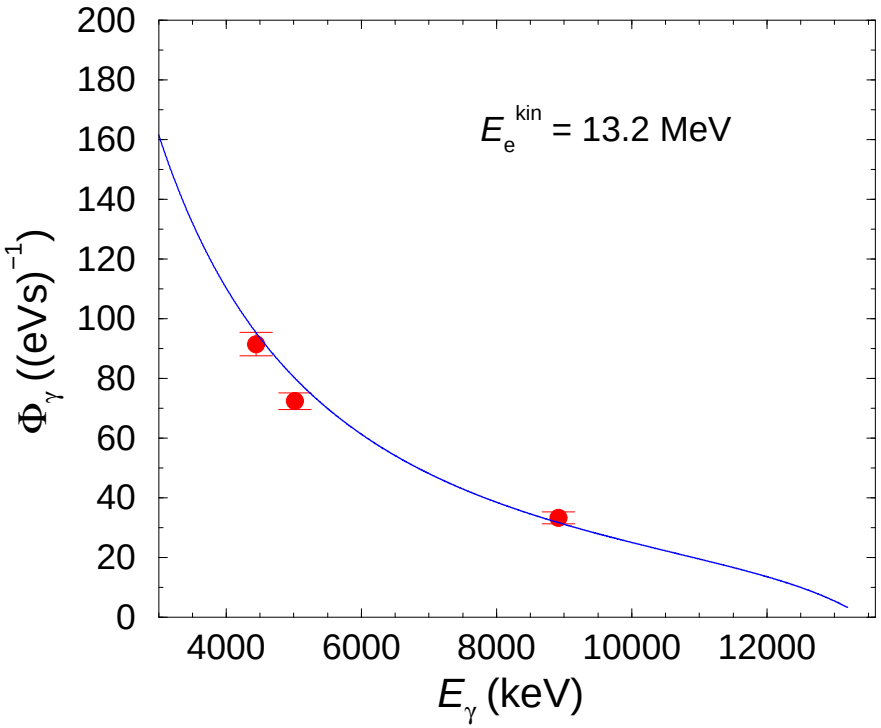

Absolute photon flux deduced from transitions in ^{11}B using the calculated efficiency shown in the left panel and relative photon flux calculated according to G. Roche et al.
Code by E. Haug, Rad. Phys. Chem. 77 (2008) 207.

Unresolved strength in the continuum

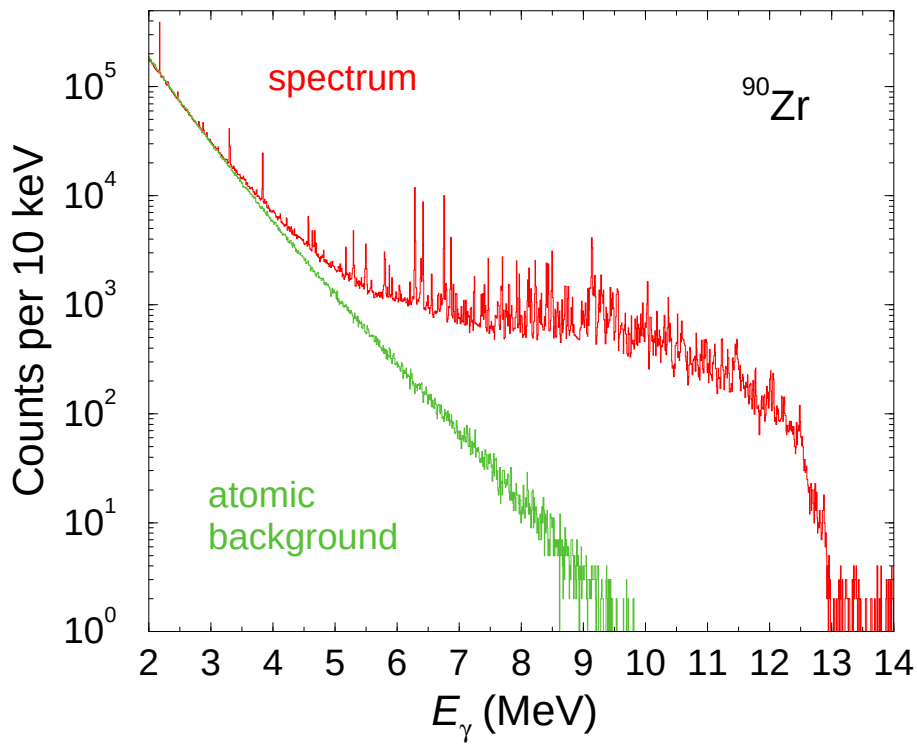

Experimental spectrum of ^{90}Zr (corrected for room background, detector response, efficiency, measuring time) and simulated spectrum of atomic background.

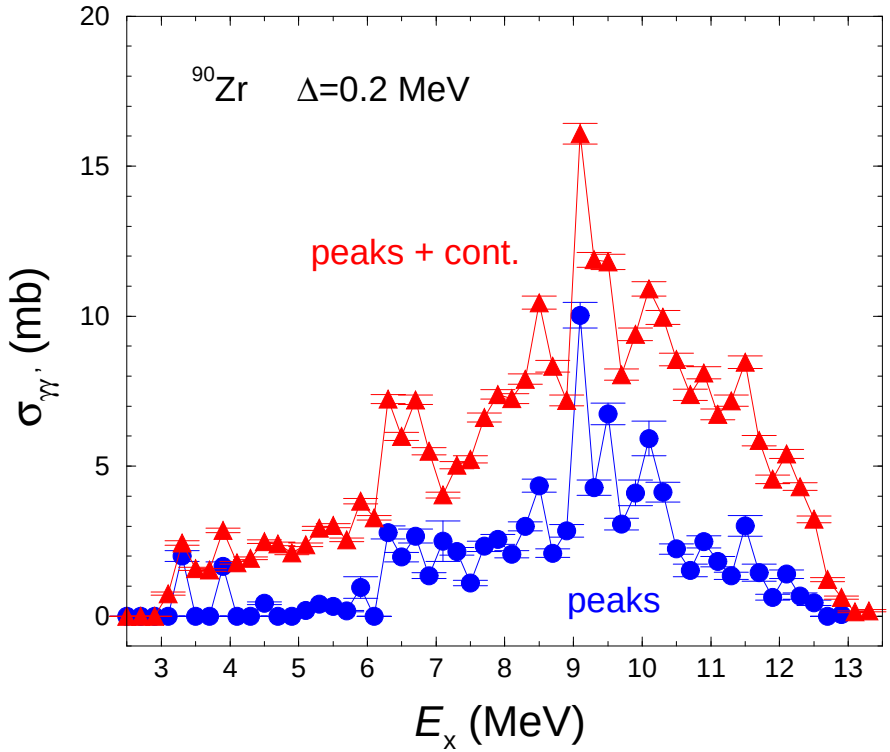

Scattering cross sections in ^{90}Zr averaged over energy bins of 0.2 MeV, not corrected for branching, derived from the difference of the experimental spectrum and the atomic background (triangles) and from the resolved peaks only (circles).

Problem of feeding and branching

Correction of the strength function by using statistical methods (G. Rusev, Dissertation):

⇒ Monte Carlo simulations of γ-ray cascades from groups of levels in 100 keV bins over the whole energy range.

⇒ Level scheme of $J = 0$, 1 and 2 states constructed using:
- Backshifted Fermi-Gas Model with level-density parameters given in:
  T. v. Egidy, D. Bucurescu, PRC 72 (2005) 044311
- Wigner level-spacing distributions

⇒ Partial decay widths calculated by using:
- Photon strength functions approximated by Lorentzian parametrisations.
  - $E1$: parameters determined from a fit to (γ,n) data
  - $M1$: global parametrisation of $M1$ spin-flip resonances
  - $E2$: global parametrisation of $E2$ isoscalar resonances
  (www-nds.iaea.org/RIPL-2)
- Porter-Thomas distributions of decay widths.

⇒ Feeding intensities subtracted and intensities of g.s. transitions corrected with calculated branching ratios Γ_0/Γ.

Simulations of γ-ray cascades

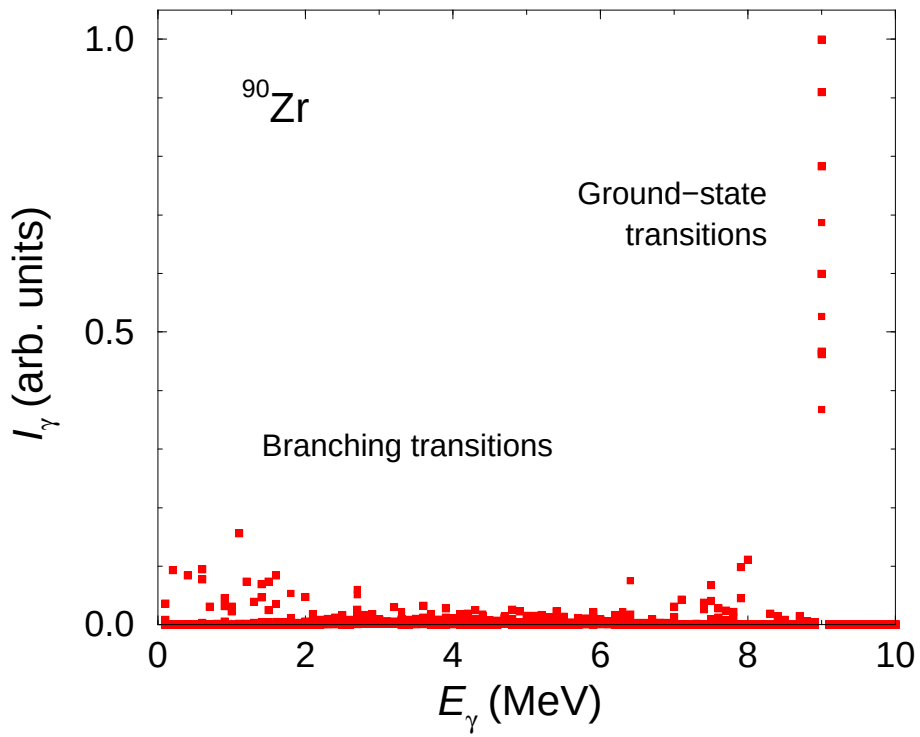

Simulated intensity distribution of transitions depopulating levels in a 100 keV bin around 9 MeV.
⇒ Subtraction of intensities of branching transitions.

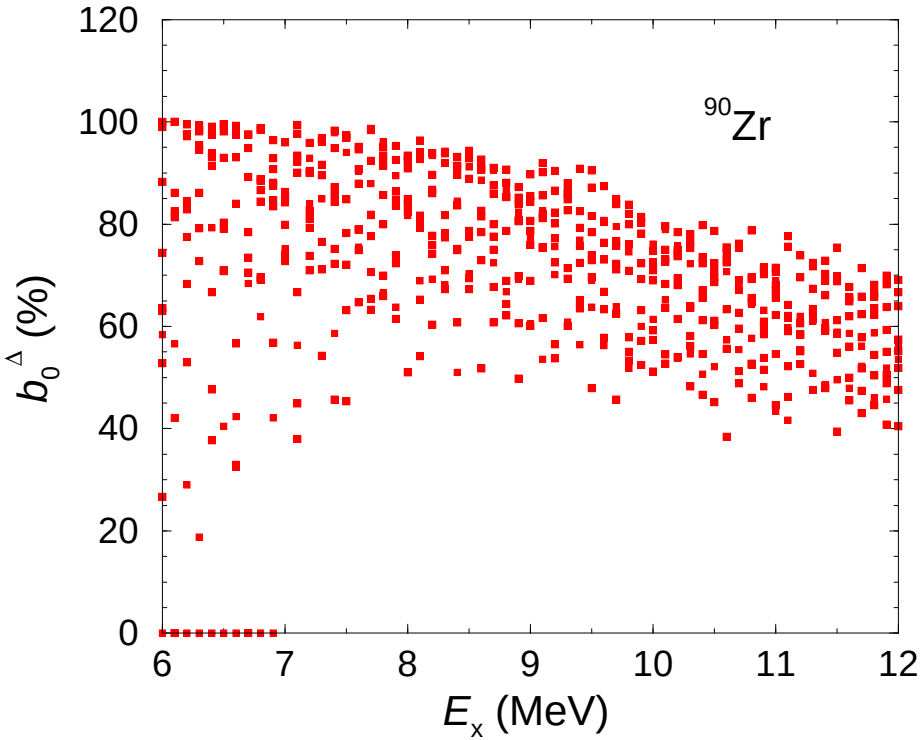

Distribution of branching ratios $b_0 = \Gamma_0/\Gamma$ versus the excitation energy as obtained from the simulations of γ-ray cascades for ^{90}Zr.
⇒ Estimate of Γ_0 and σ_γ.

Test of simulated branching ratios

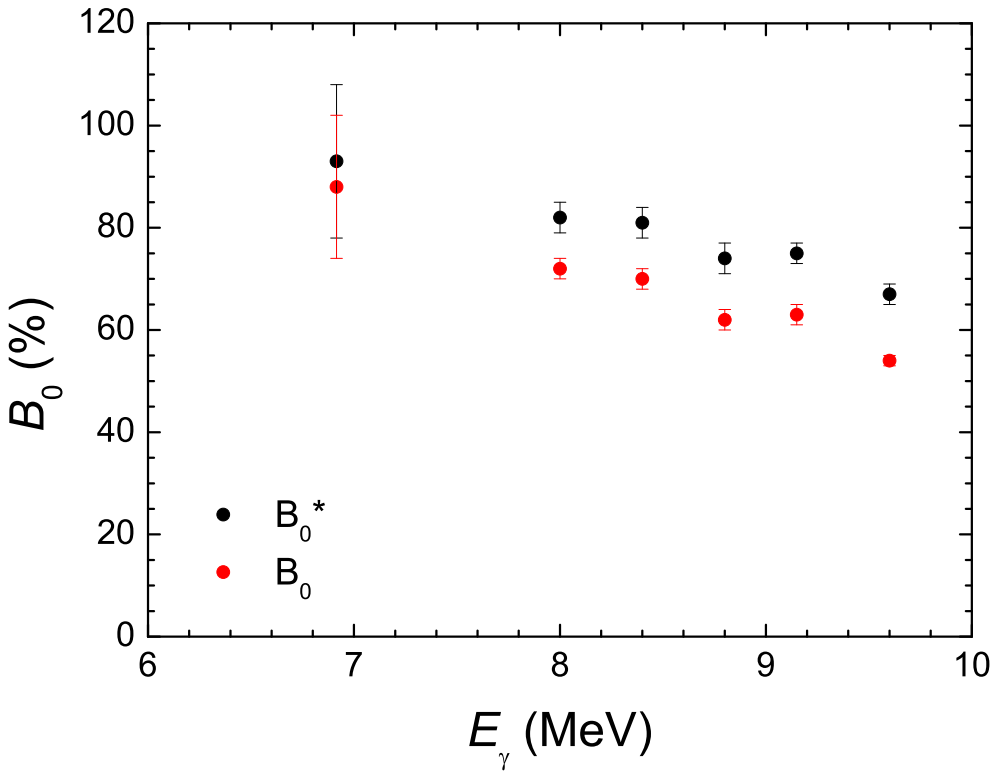

Measurement with monochromatic photons at HIγS ($\Delta E \approx$ 200 keV).
Black: Population of 0_2^+ neglected.
Red: Assumption that $b_{0_2^+} = b_{2_1^+}$.
G. Rusev, A.P. Tonchev et al., priv. comm.

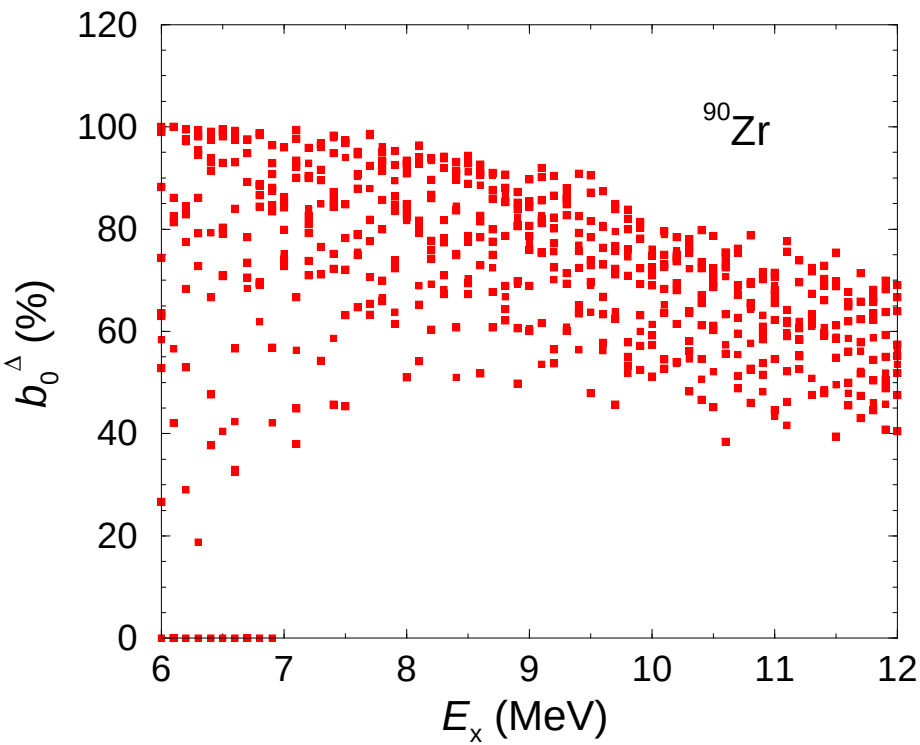

Distribution of branching ratios $b_0 = \Gamma_0/\Gamma$ versus the excitation energy as obtained from the simulations of γ-ray cascades for ^{90}Zr.

Test of E1 strength functions

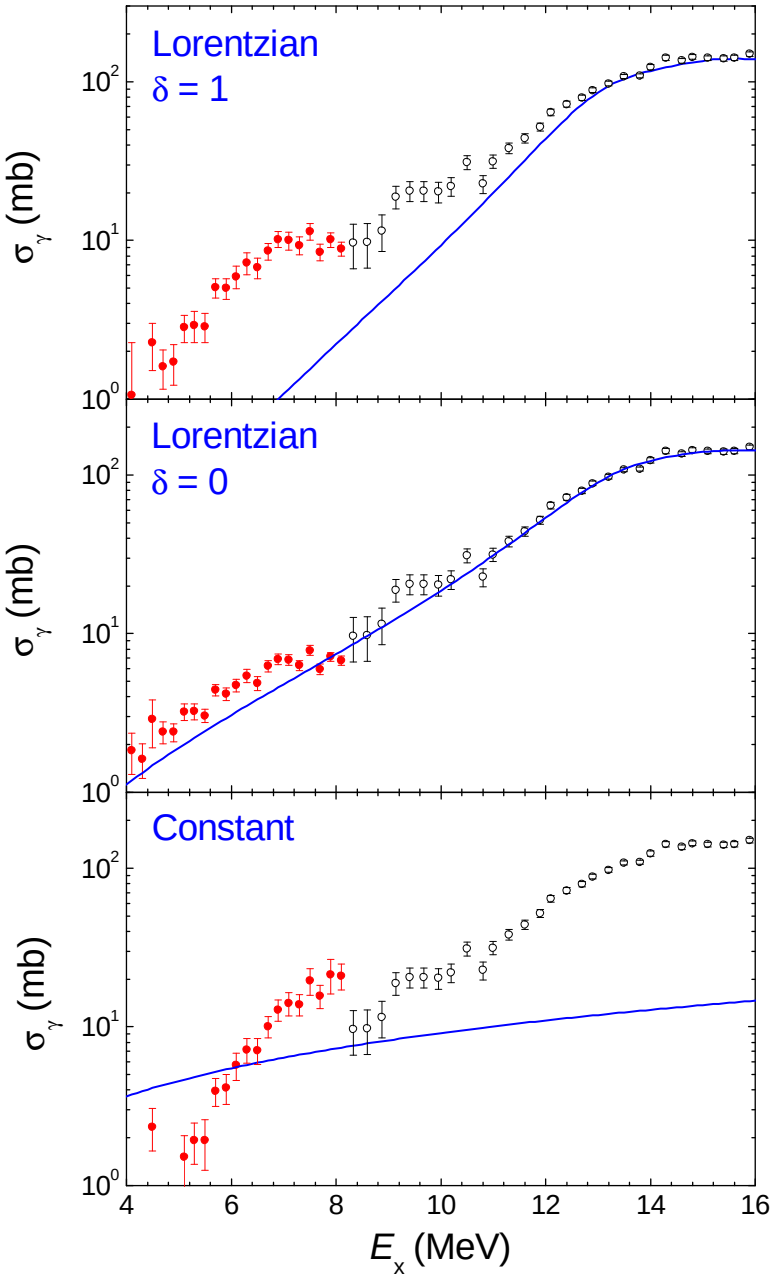

$$\sigma_\gamma(E_x) = \frac{2S_{\mathrm{TRK}}}{3\pi} \sum_{i=1}^{3} \frac{E_x^2 \Gamma_i(E_x)}{(E_i^2 - E_x^2)^2 + E_x^2 \Gamma_i^2(E_x)}$$

$$\Gamma_i(E_x) = \Gamma_S \cdot (E_x/E_i)^\delta; \quad \Gamma_S = 4 \text{ MeV};$$

$$f_1 = \sigma_\gamma / [3(\pi\hbar c)^2 E_\gamma]$$

$$S_{\mathrm{TRK}} = \int_0^\infty \sigma_\gamma(E)\, dE = 60 \frac{NZ}{A} \text{ MeV mb}$$

$$E_i = \hbar\omega_0 \left(1 - \frac{2}{3}\epsilon_2 \cos\left(\gamma - \frac{2\pi i}{3}\right)\right)$$

Absorption cross section in ^{90}Zr

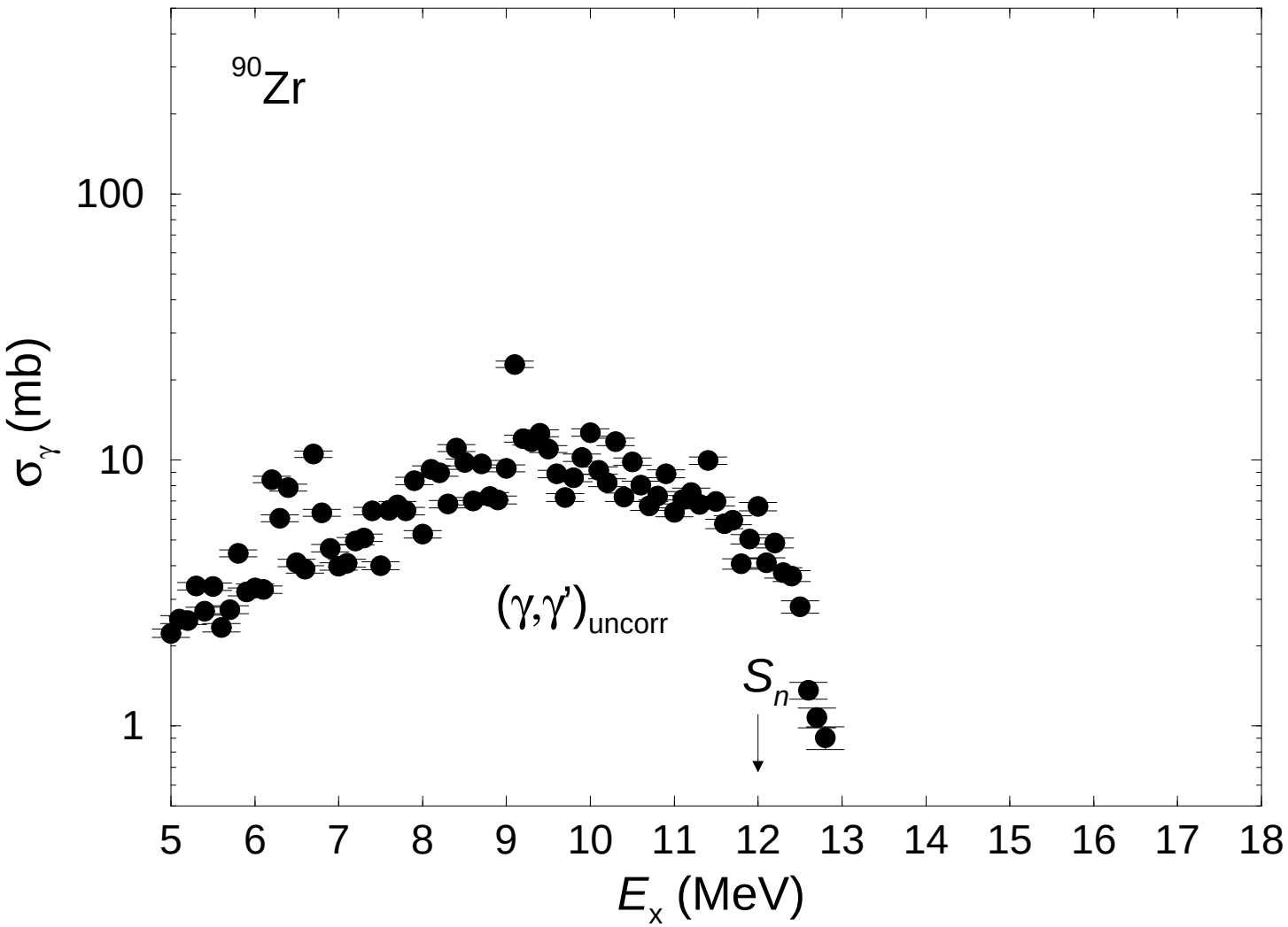

Present (γ, γ) data

Absorption cross section in ^{90}Zr

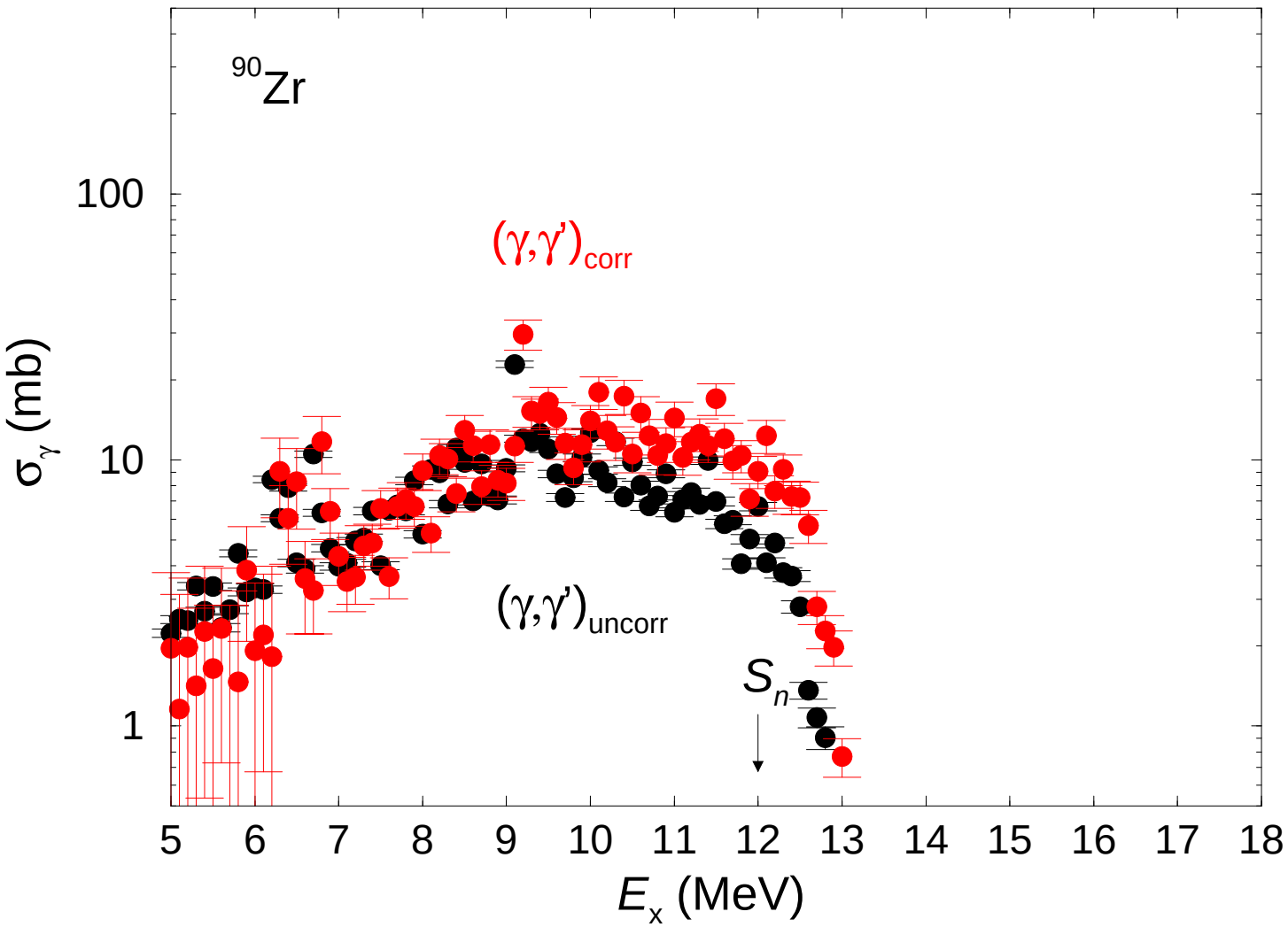

Present (γ, γ) data

Absorption cross section in ^{90}Zr

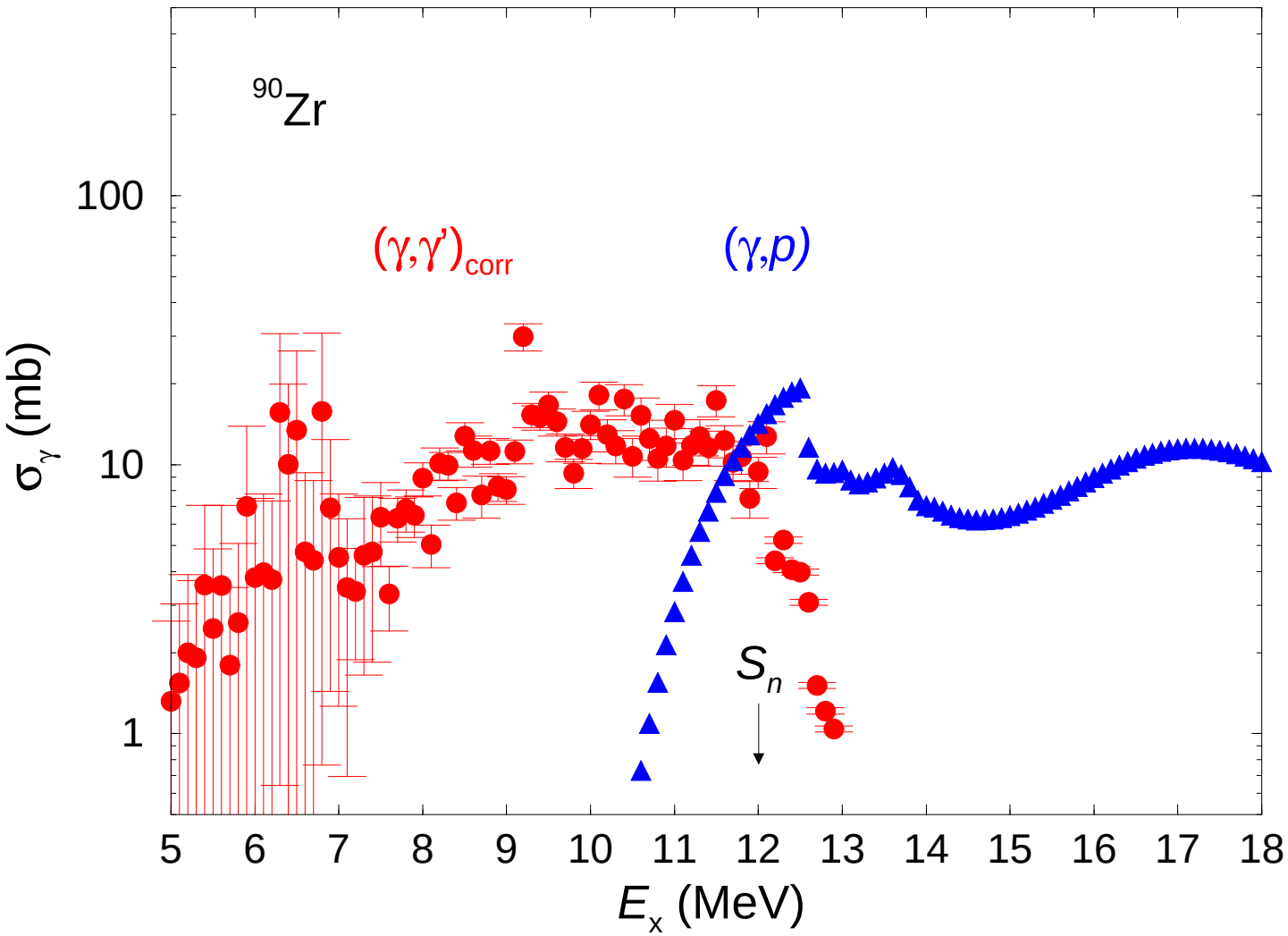

Present (γ, γ) data

(γ, p) calculated
ADNDT 88 (2004) 1

Absorption cross section in ^{90}Zr

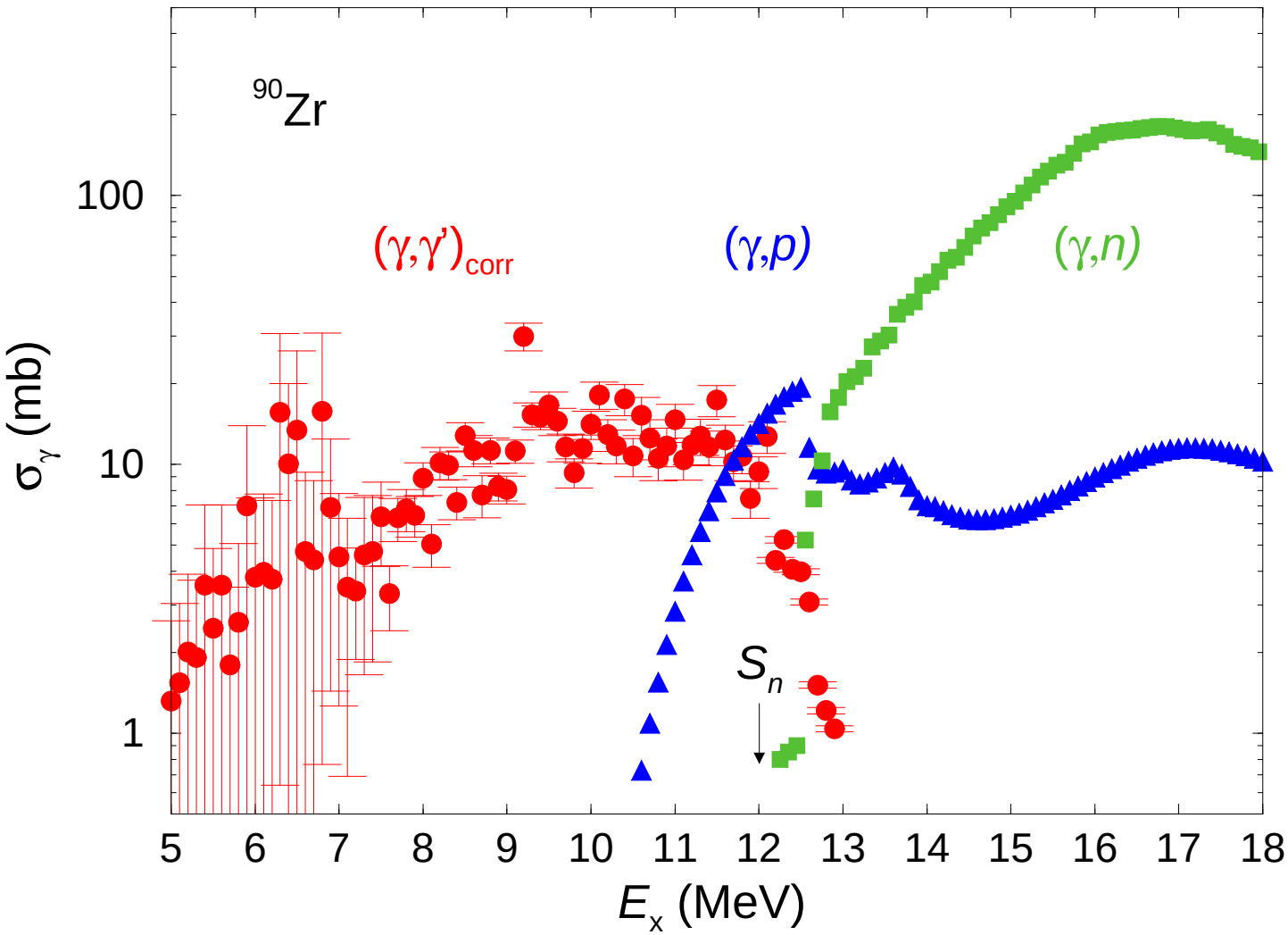

Present (γ, γ) data

(γ, p) calculated
ADNDT 88 (2004) 1

(γ, n) data
PR 162 (1967) 1098

Absorption cross section in ^{90}Zr

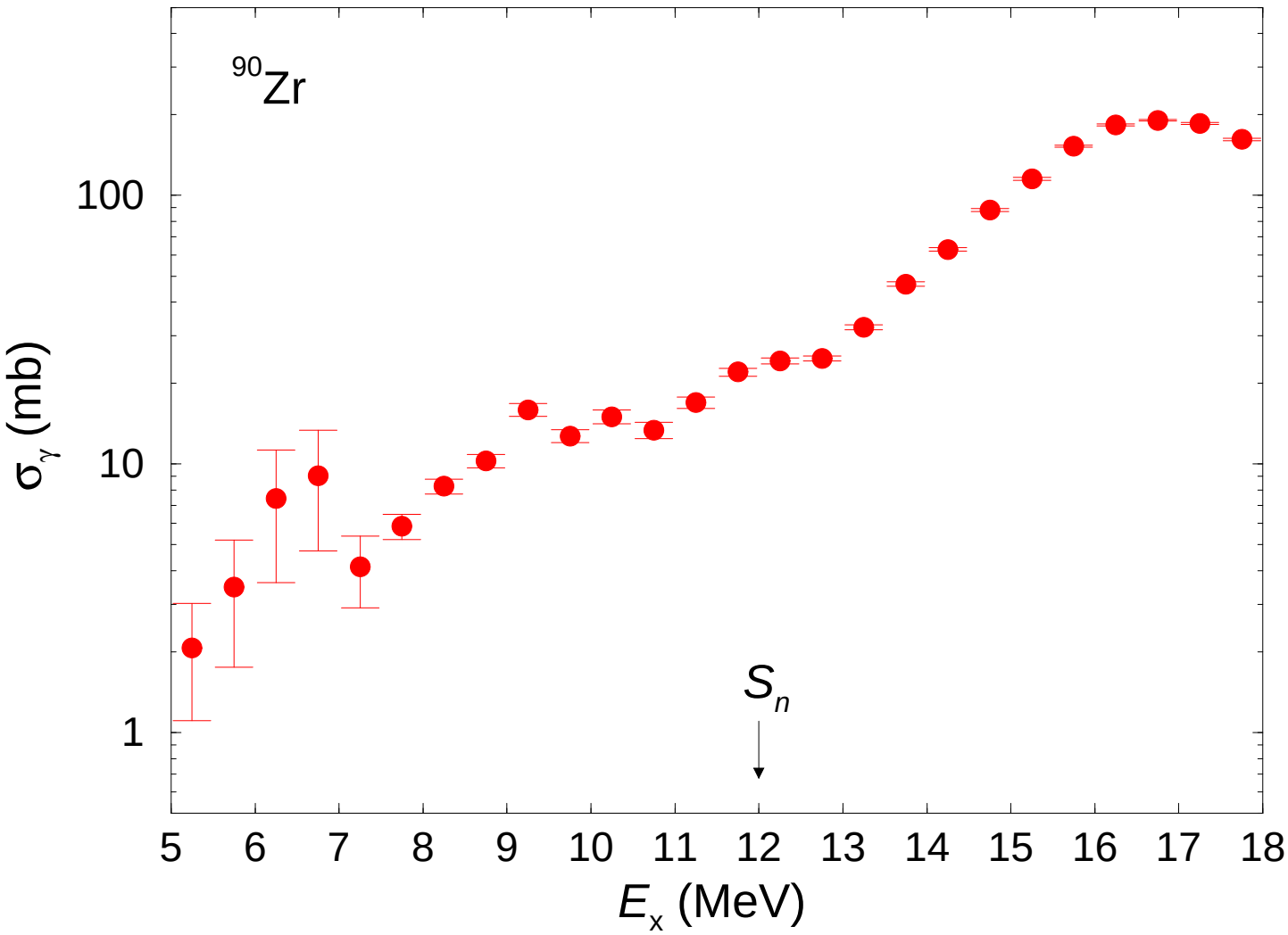

Present (γ, γ) data
$+ (\gamma, p) + (\gamma, n)$ data

Absorption cross section in ^{90}Zr

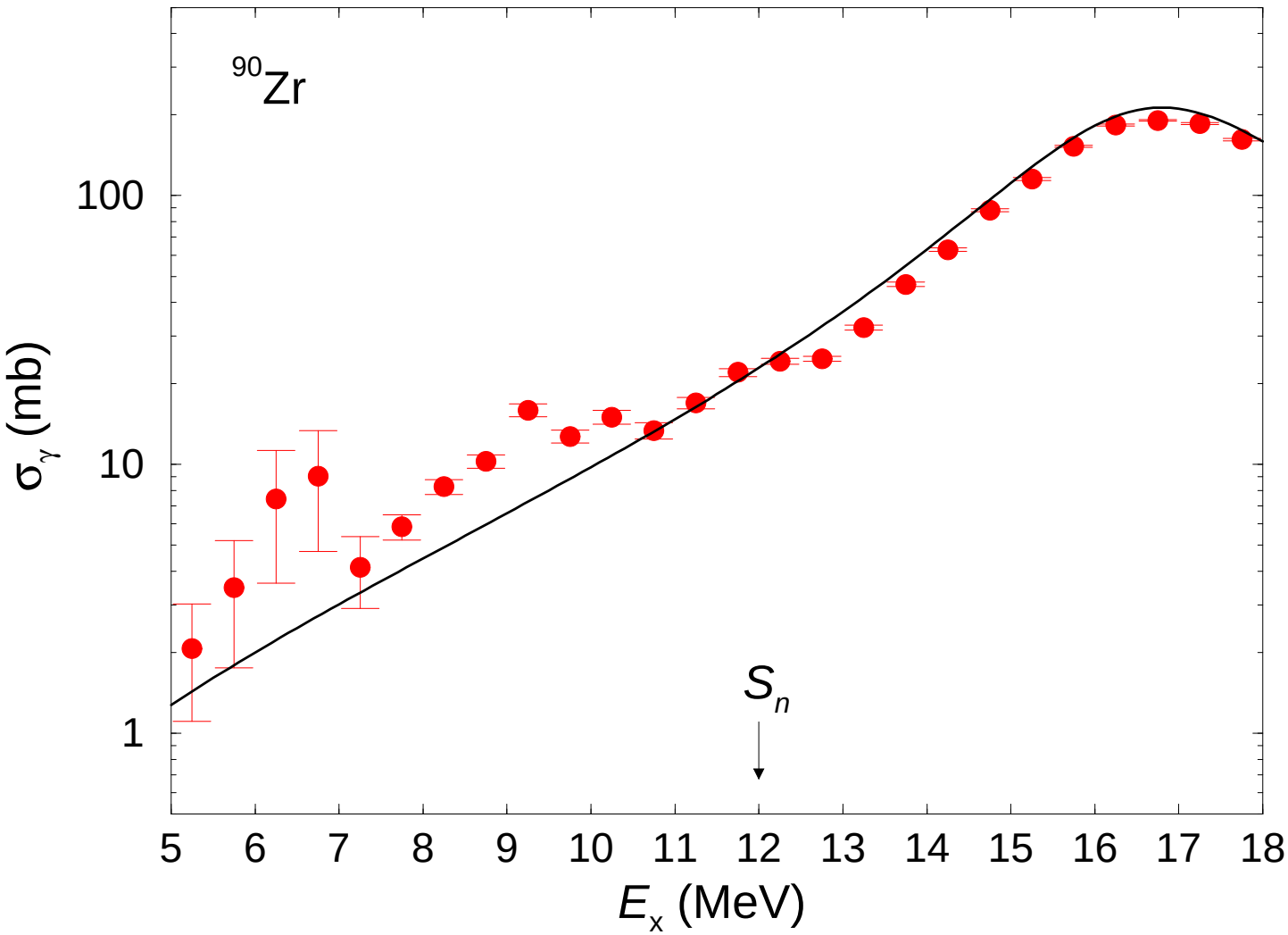

Present (γ, γ) data
$+ (\gamma, p) + (\gamma, n)$ data

Lorentz curve:

$E_0 = 16.8$ MeV

$\Gamma = 4.0$ MeV

$\frac{\pi}{2}\sigma_0\Gamma = 60\ \frac{NZ}{A}$ MeV mb

Absorption cross section in ^{90}Zr

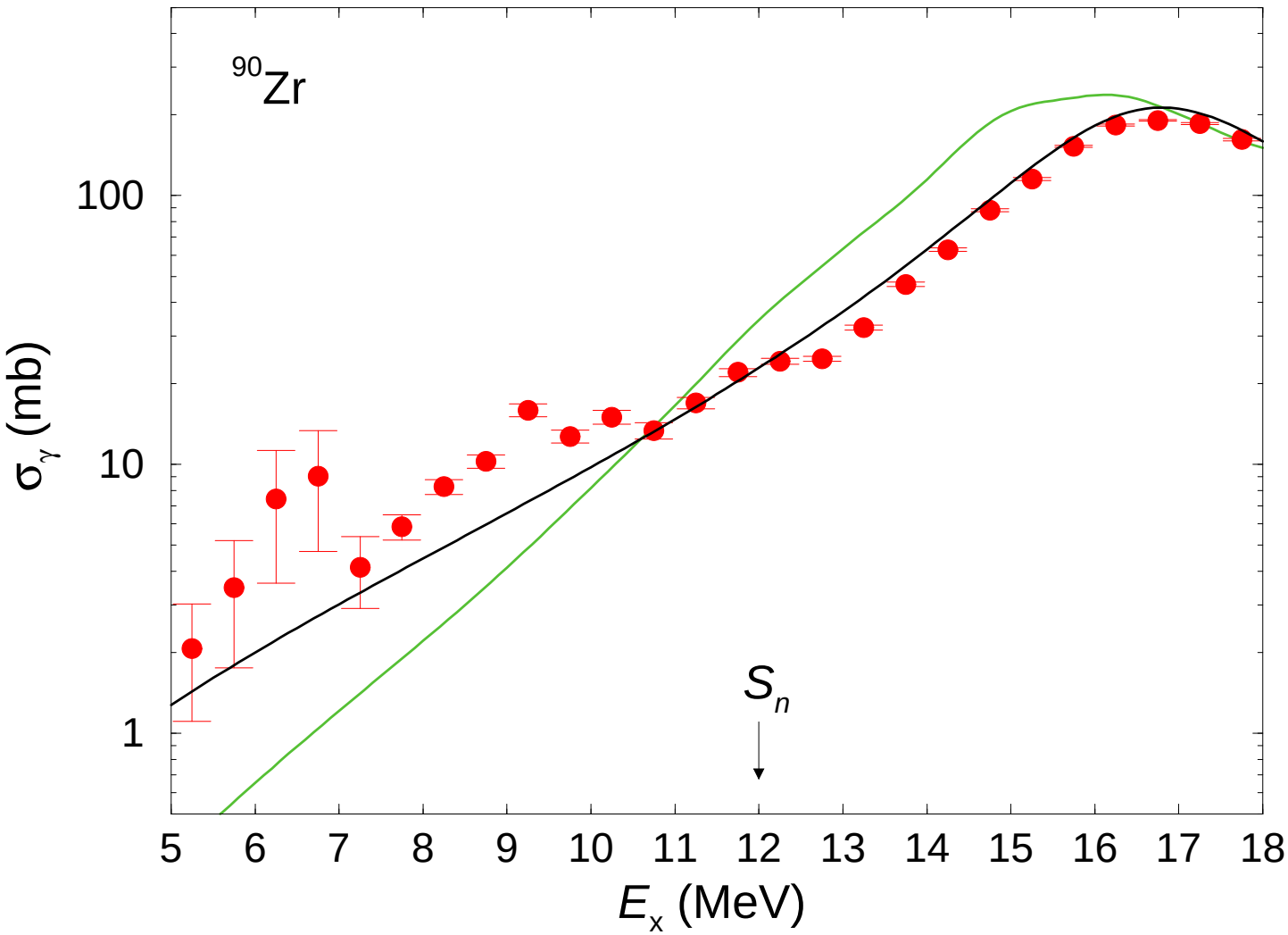

Present (γ, γ) data
$+ (\gamma, p) + (\gamma, n)$ data

Lorentz curve:

$E_0 = 16.8$ MeV

$\Gamma = 4.0$ MeV

$\frac{\pi}{2}\sigma_0\Gamma = 60\ \frac{NZ}{A}$ MeV mb

RIPL-2
(S. Goriely, E. Khan,
NPA 706 (2002) 217)

Absorption cross section in ^{90}Zr

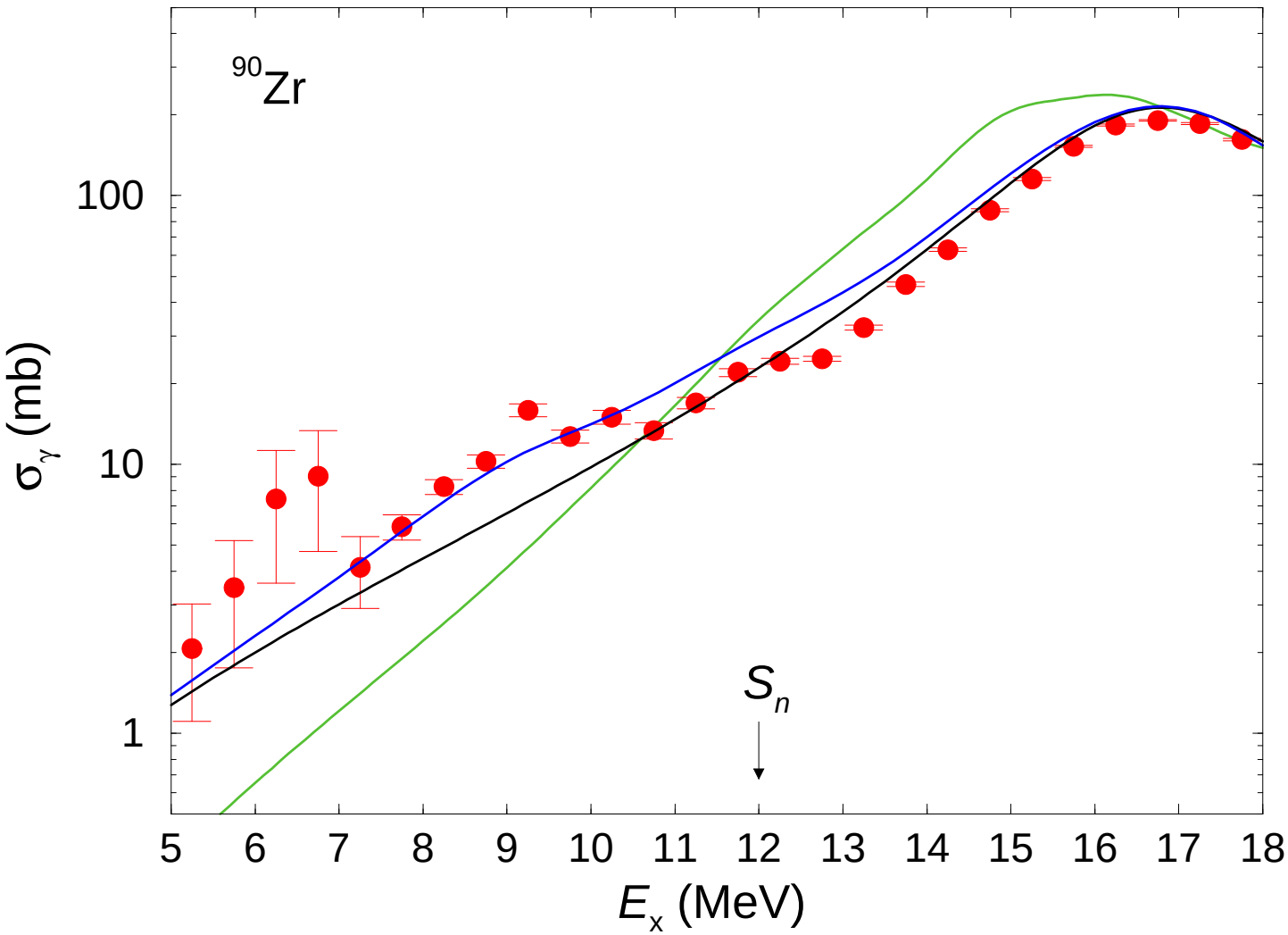

Present (γ, γ) data
$+ (\gamma, p) + (\gamma, n)$ data

Lorentz curve:

$E_0 = 16.8$ MeV

$\Gamma = 4.0$ MeV

$\frac{\pi}{2}\sigma_0\Gamma = 60\ \frac{NZ}{A}$ MeV mb

RIPL-2
(S. Goriely, E. Khan,
NPA 706 (2002) 217)

QRPA
Woods-Saxon basis
$\Gamma = 3.2$ MeV

Absorption cross section in ^{88}Sr

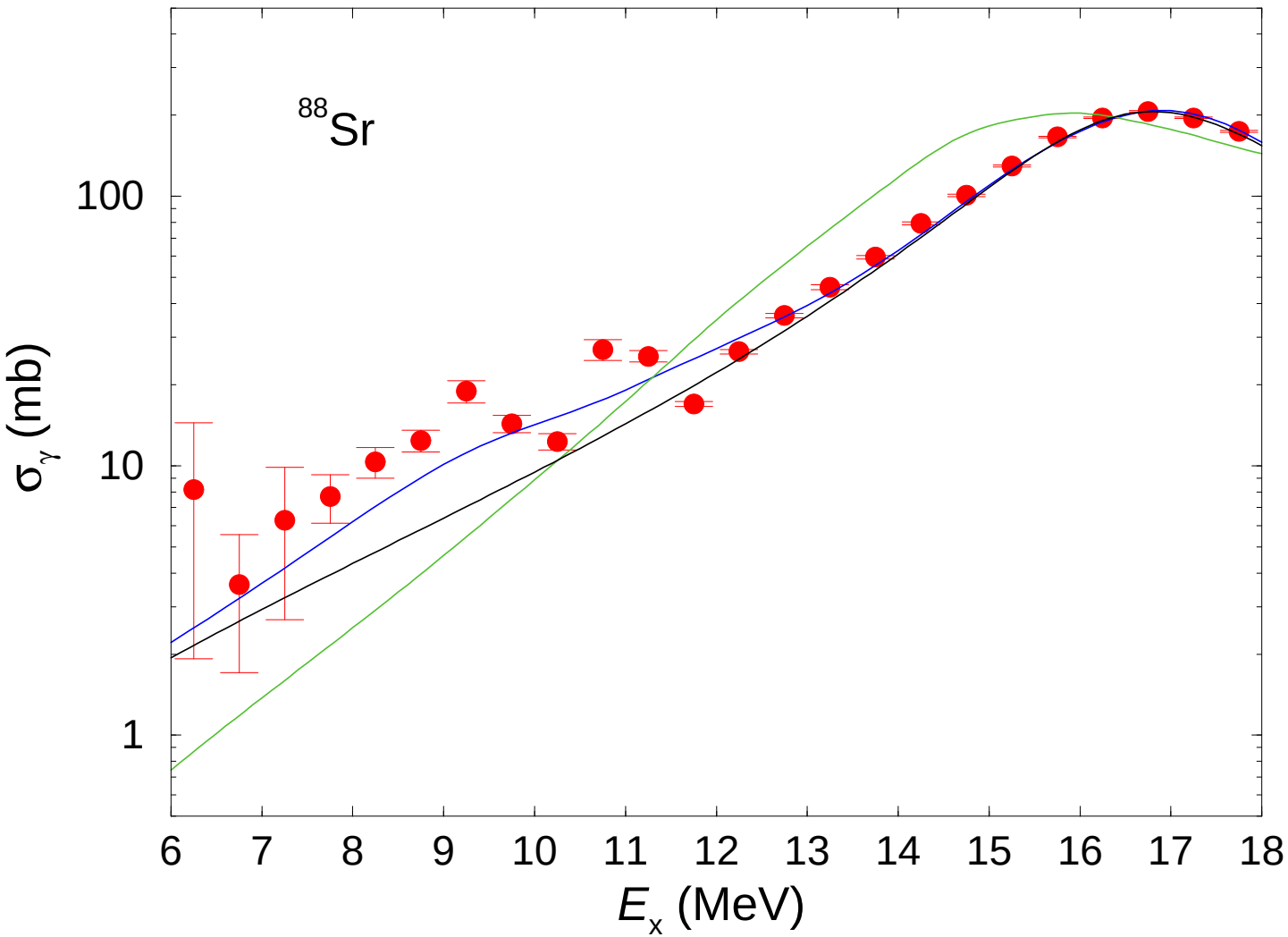

Present (γ, γ) data
$+ (\gamma, n)$ data

Lorentz curve:

$E_0 = 16.8$ MeV

$\Gamma = 4.0$ MeV

$\frac{\pi}{2}\sigma_0\Gamma = 60\ \frac{NZ}{A}$ MeV mb

RIPL-2
(S. Goriely, E. Khan,
NPA 706 (2002) 217)

QRPA
Woods-Saxon basis:
$\Gamma = 3.2$ MeV

Absorption cross section in ^{89}Y

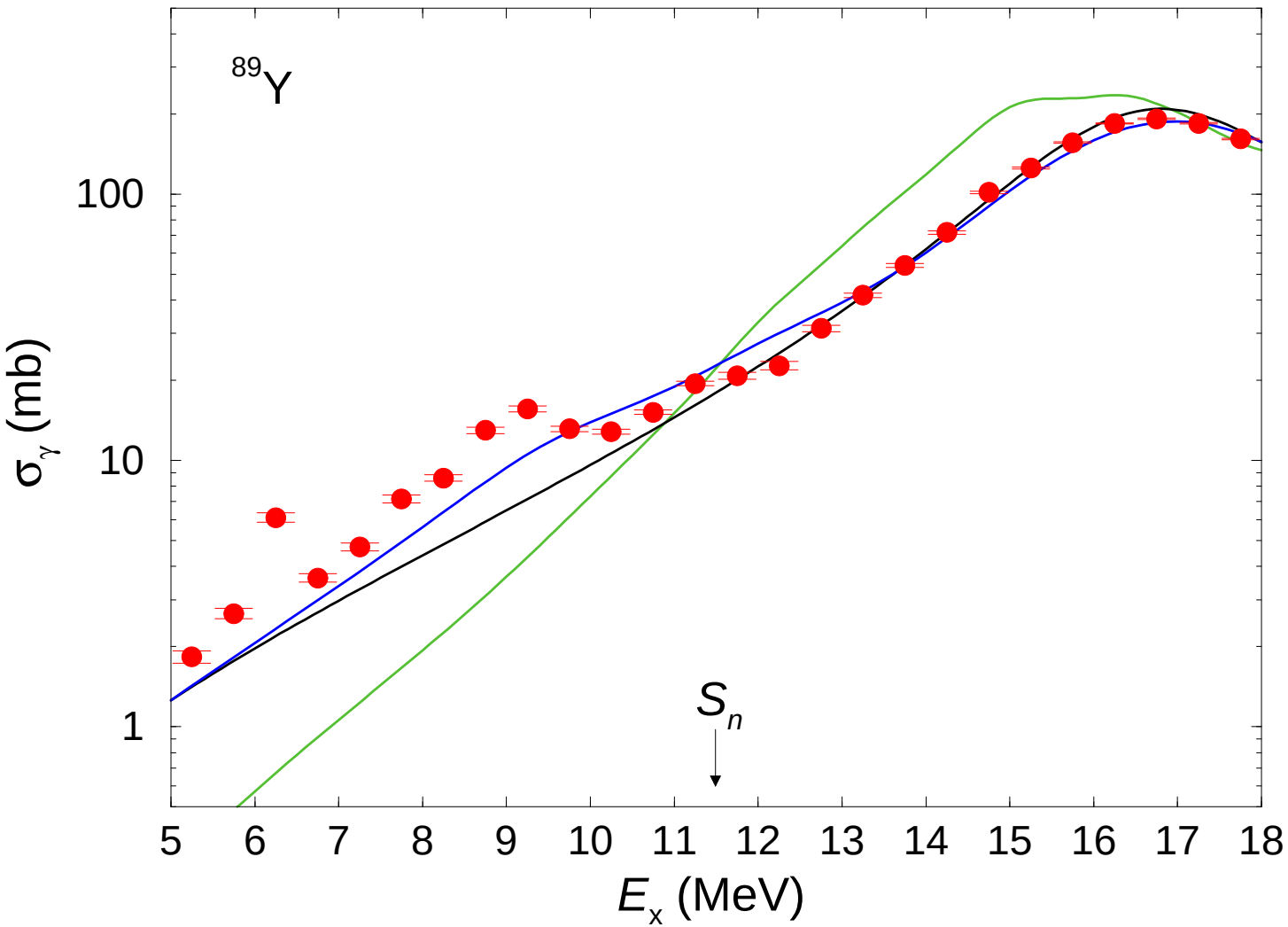

Present (γ, γ) data
$+ (\gamma, p) + (\gamma, n)$ data

Lorentz curve:

$E_0 = 16.8$ MeV

$\Gamma = 4.0$ MeV

$\frac{\pi}{2}\sigma_0\Gamma = 60\ \frac{NZ}{A}$ MeV mb

RIPL-2
(S. Goriely, E. Khan,
NPA 706 (2002) 217)

QRPA
Woods-Saxon basis:
$\Gamma = 3.2$ MeV

One-phonon QPM calculations for ^{88}Sr and ^{90}Zr

Transition densities of neutrons and protons:

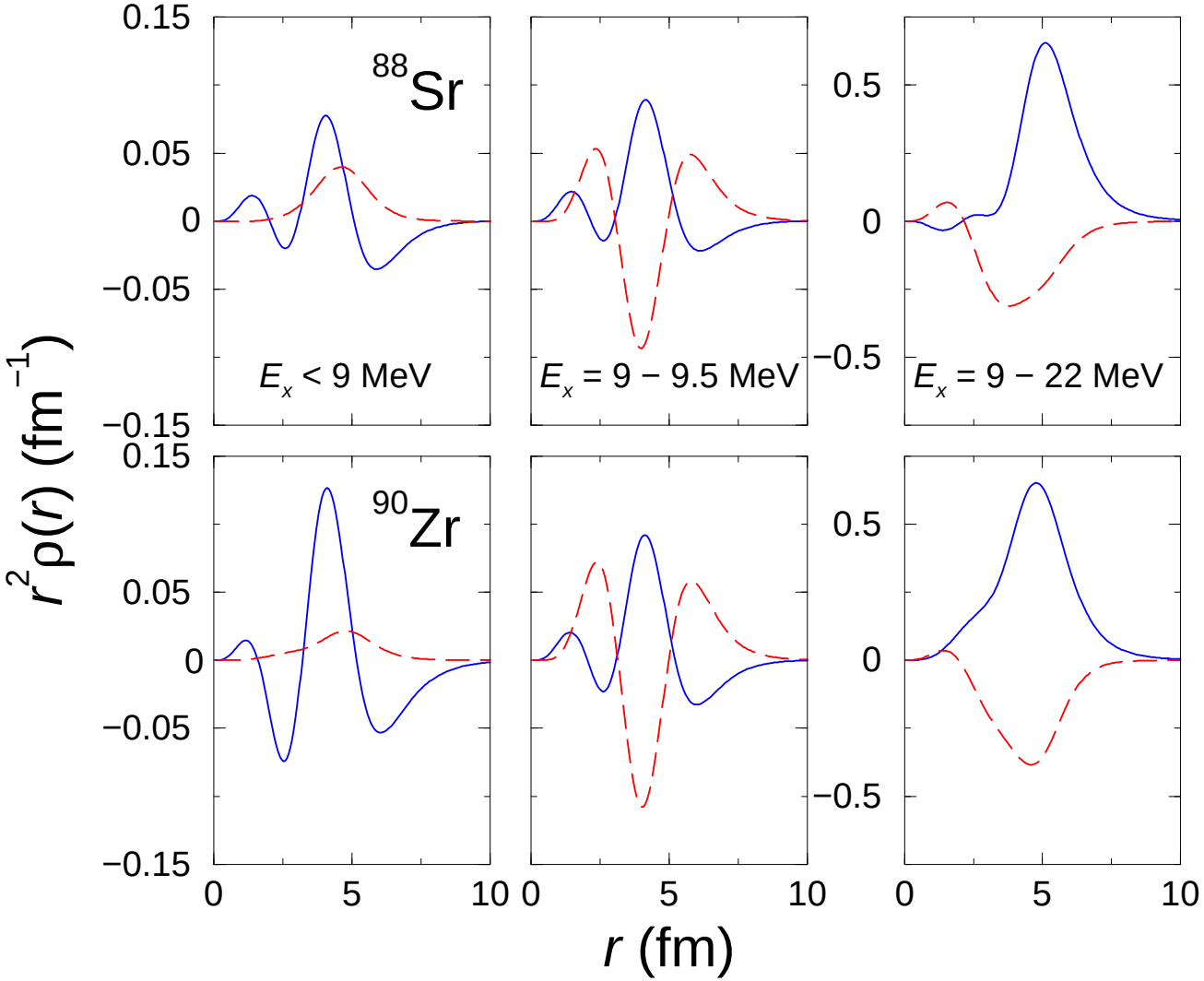

Energy range below 9 MeV:

⇒ Oscillations at the surface by neutrons only

⇒ Indication for a PDR

Absorption cross sections in Mo isotopes

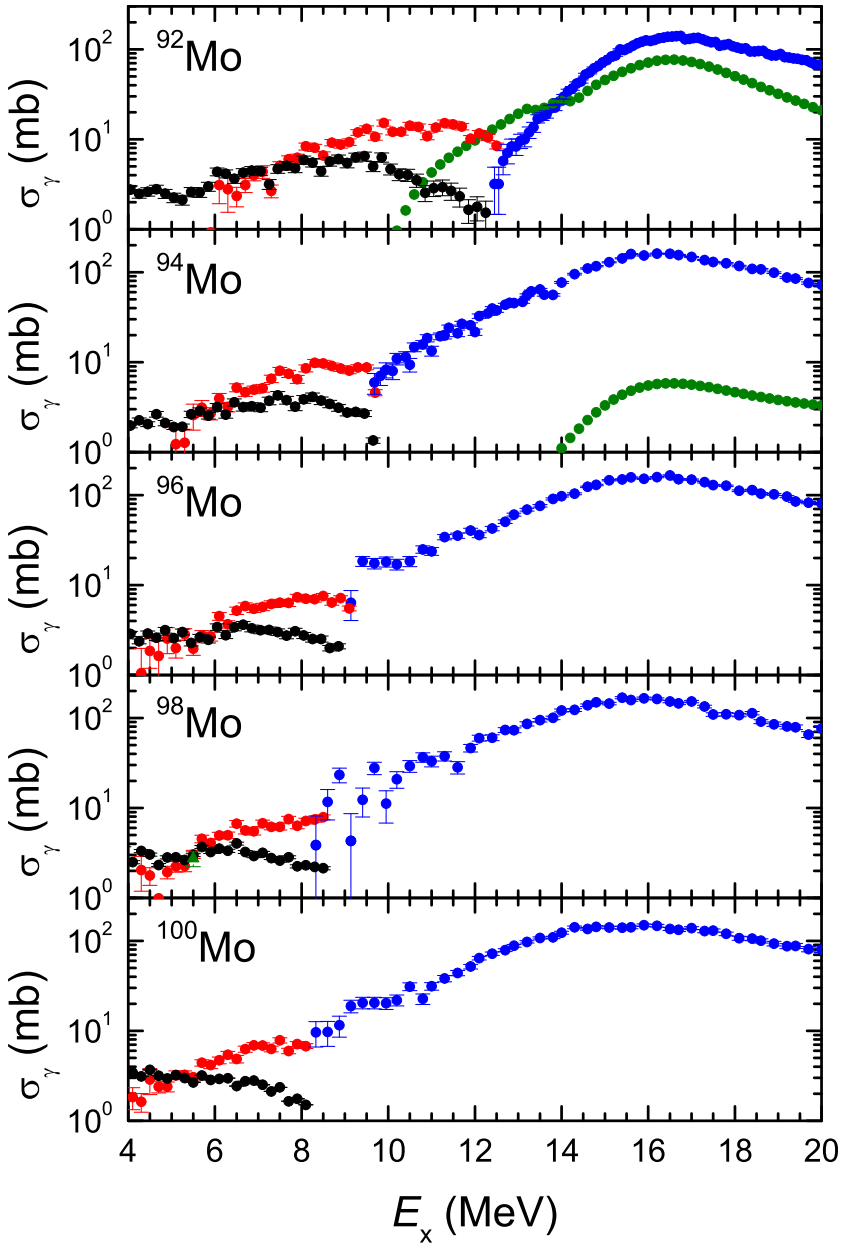

$$\sigma_\gamma(E_x) = \frac{2S_{\mathrm{TRK}}}{3\pi} \sum_{i=1}^{3} \frac{E_x^2 \Gamma_i(E_x)}{(E_i^2 - E_x^2)^2 + E_x^2 \Gamma_i^2(E_x)}$$

$$\Gamma_i(E_x) = \Gamma_S \cdot (E_x/E_i)^\delta; \quad \Gamma_S = 4 \text{ MeV}; \quad \delta \approx 0$$

$$S_{\mathrm{TRK}} = \int_0^\infty \sigma_\gamma(E)\, dE = 60 \frac{NZ}{A} \text{ MeV mb}$$

$$E_i = \hbar\omega_0 \left(1 - \frac{2}{3}\epsilon_2 \cos\left(\gamma - \frac{2\pi i}{3}\right)\right)$$

Absorption cross sections in Mo isotopes

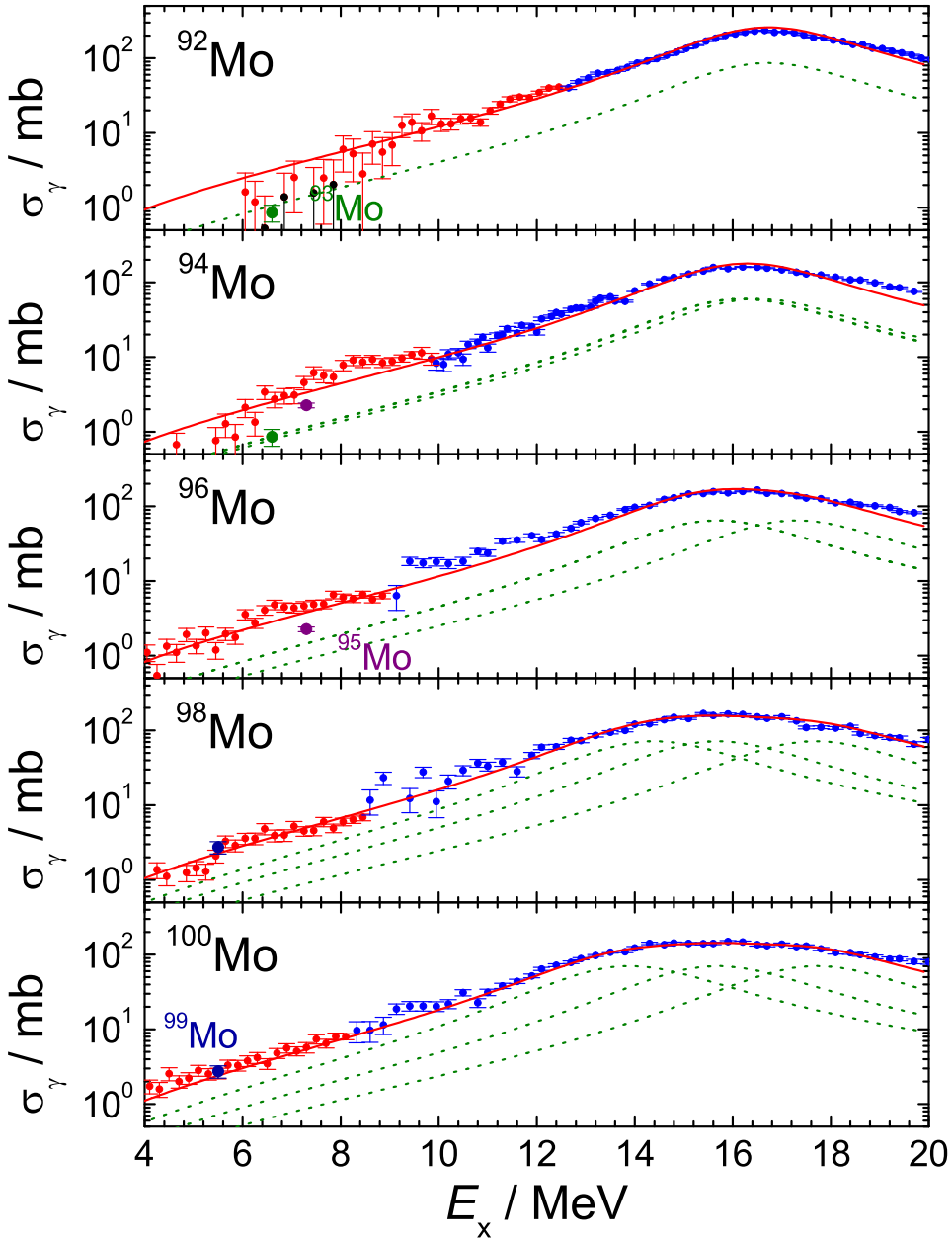

$$\sigma_\gamma(E_x) = \frac{2S_{\mathrm{TRK}}}{3\pi} \sum_{i=1}^{3} \frac{E_x^2 \Gamma_i(E_x)}{(E_i^2 - E_x^2)^2 + E_x^2 \Gamma_i^2(E_x)}$$

$$\Gamma_i(E_x) = \Gamma_S \cdot (E_x/E_i)^\delta; \quad \Gamma_S = 4 \text{ MeV}; \quad \delta \approx 0$$

$$S_{\mathrm{TRK}} = \int_0^\infty \sigma_\gamma(E)\, dE = 60 \frac{NZ}{A} \text{ MeV mb}$$

$$E_i = \hbar\omega_0 \left(1 - \frac{2}{3}\epsilon_2 \cos\left(\gamma - \frac{2\pi i}{3}\right)\right)$$

Comparison with other experiments

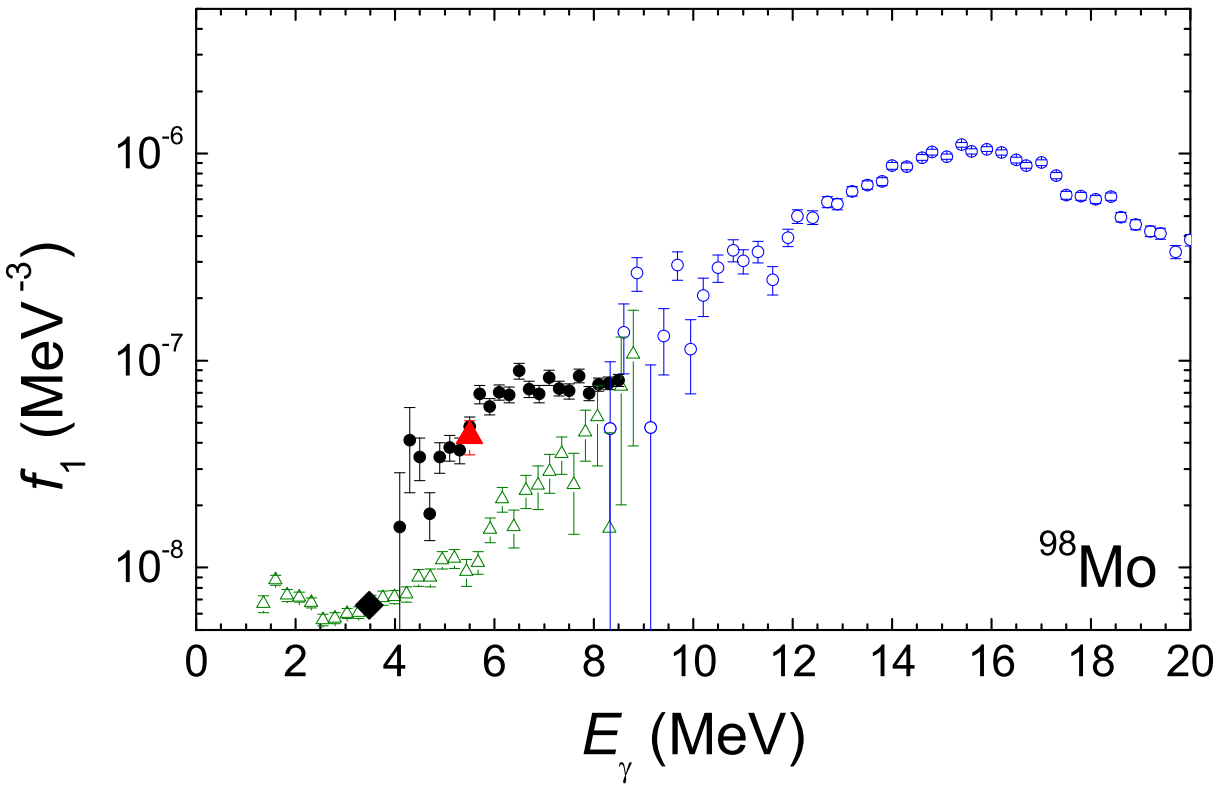

Present (γ, γ) data

(γ, n) data

H. Beil et al., NPA 227 (1974) 427

(^{3}He,^{3}He'γ) data

M. Guttormsen et al., PRC 71 (2005) 044307

(n, γ) data

J. Kopecky and M. Uhl, Bologna 1994

QRPA calculations for deformed nuclei

Hamiltonian for 1^- states:

- Nilsson or Woods-Saxon mean field plus monopole pairing
- isoscalar and isovector dipole-dipole and octupole-octupole interactions

F. Dönau, PRL 94 (2005) 092503

F. Dönau et al., PRC 76 (2007) 014317

Total energy as a function of the quadrupole deformation ε_2 and the triaxiality γ:

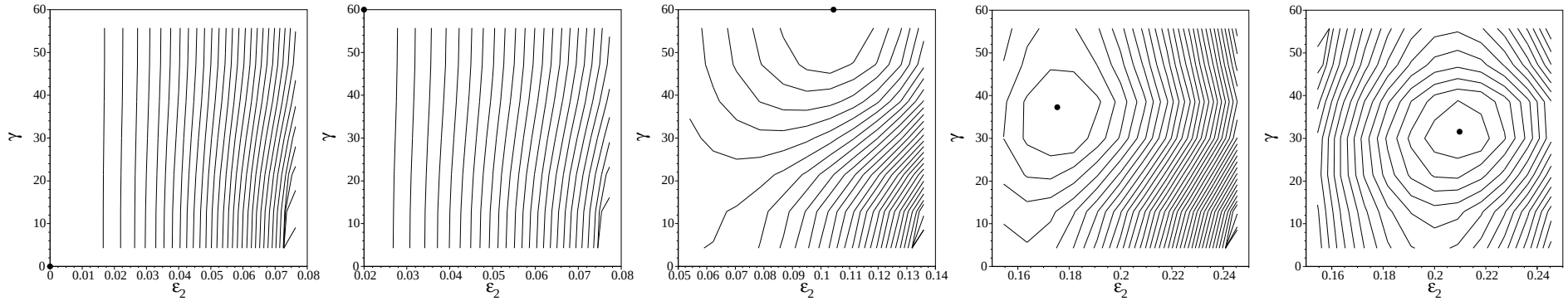

$^{92}Mo_{50}$	$^{94}Mo_{52}$	$^{96}Mo_{54}$	$^{98}Mo_{56}$	$^{100}Mo_{58}$
$\varepsilon_2 = 0.0$	$\varepsilon_2 = 0.02$	$\varepsilon_2 = 0.10$	$\varepsilon_2 = 0.18$	$\varepsilon_2 = 0.21$
		$\gamma = 60°$	$\gamma = 37°$	$\gamma = 32°$

TAC model with shell-correction method:

S. Frauendorf, NPA 557 (1993) 259c, NPA 667 (2000) 115

QRPA calculations in a deformed basis for Mo isotopes

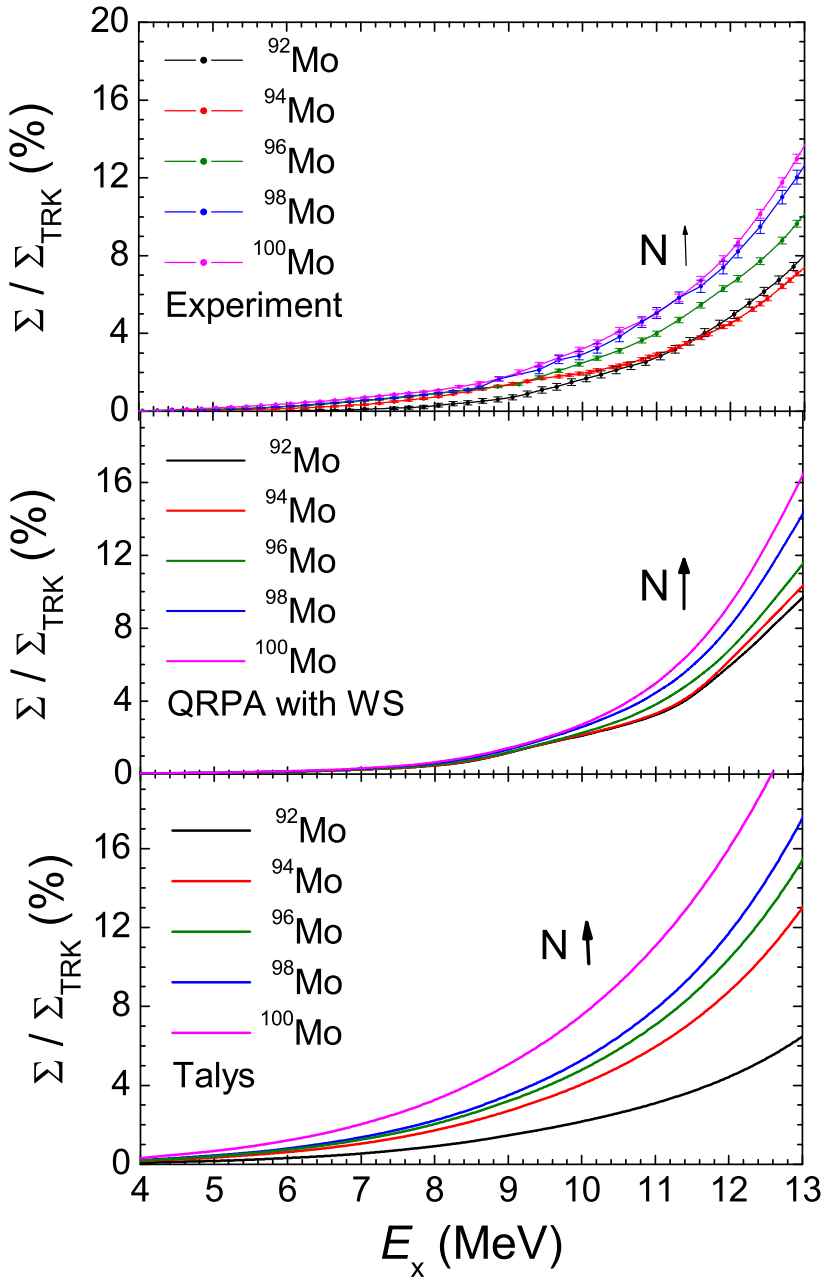

$$\Sigma(E_x) = \sum_{i}^{E_x} \sigma_\gamma(E_i)\ \Delta E$$

$$\Sigma_{TRK} = \int_0^\infty \sigma_\gamma(E)\ dE = 60\frac{NZ}{A}\ \text{MeV mb}$$

Summary

- Study of dipole-strength distributions at high excitation energy and high level density via photon scattering.
- Comparison of measured spectrum with calculated atomic background: 30 – 40% of the total dipole strength in resolved peaks and 70 – 60% in continuum.
- Simulations of statistical γ cascades: Estimate of intensities of inelastic transitions.
- Deduced σ_γ connect smoothly with (γ,n) data.

⇒ (i) Correct determination of σ_γ up to the (γ,n) threshold.
(ii) Information on the photoabsorption cross section over the whole energy range from low excitation energy up to the GDR.
(iii) Observation of extra strength in the range from 6 to 12 MeV – not described in current approximations of dipole-strength functions.

⇒ QPM calculations:
(i) Qualitative description of the observed extra strength.
(ii) Extra strength below 9 MeV caused by oscillations of the excessive neutrons.
(iii) Increase of dipole strength below the neutron-threshold toward the heavier Mo isotopes is correlated with increasing deformation.

Photodissociation

Photodissociation reactions:

- (γ, n)
- (γ, p)
- (γ, α)

Method: photoactivation

- $(A, Z) + \gamma \Rightarrow (A, Z - 1) + p$
- Measure decay rate of $(A, Z - 1)$

$$N_{\mathrm{act}}(E_{\mathrm{e}}) = N_{\mathrm{tar}} \cdot \int_{E_{\mathrm{thr}}}^{E_{\mathrm{e}}} \sigma_{(\gamma,x)} \; \Phi_{\gamma}(E, E_{\mathrm{e}}) \; dE$$

$$N_{\mathrm{act}}(E_{\mathrm{e}}) = I_{\gamma}(E_{\gamma}) \cdot \varepsilon^{-1}(E_{\gamma}) \cdot p^{-1}(E_{\gamma}) \cdot \kappa_{\mathrm{corr}}$$

Photoactivation of ^{92}Mo

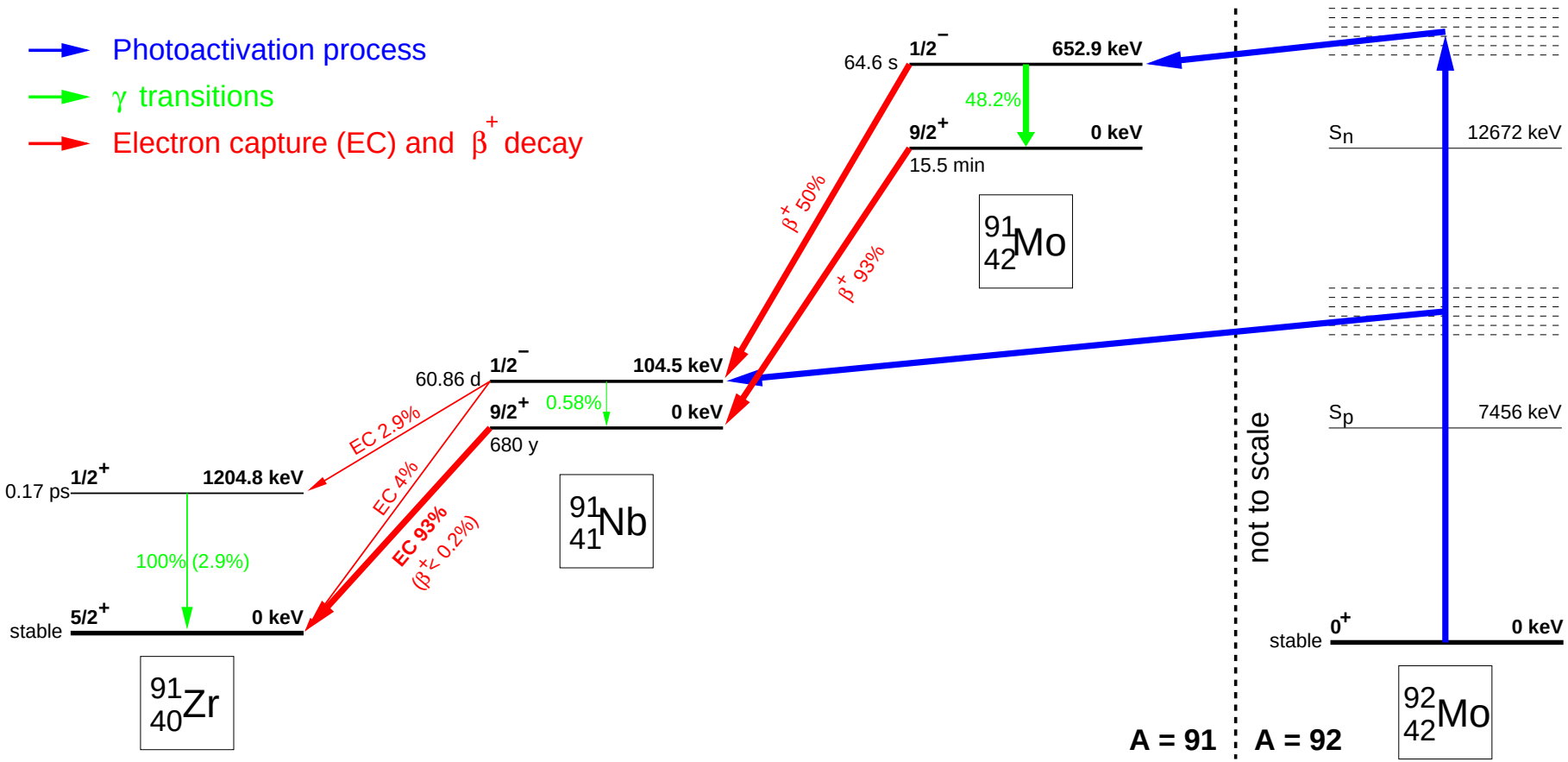

$$N_{\mathrm{act}}(E_{\mathrm{e}}) = N_{\mathrm{tar}} \cdot \int_{E_{\mathrm{thr}}}^{E_{\mathrm{e}}} \sigma_{(\gamma,x)} \; \Phi_{\gamma}(E, E_{\mathrm{e}}) \; dE$$

$$N_{\mathrm{act}}(E_{\mathrm{e}}) = I_{\gamma}(E_{\gamma}) \cdot \varepsilon^{-1}(E_{\gamma}) \cdot p^{-1}(E_{\gamma}) \cdot \kappa_{\mathrm{corr}}$$

Setup for photoactivation experiments

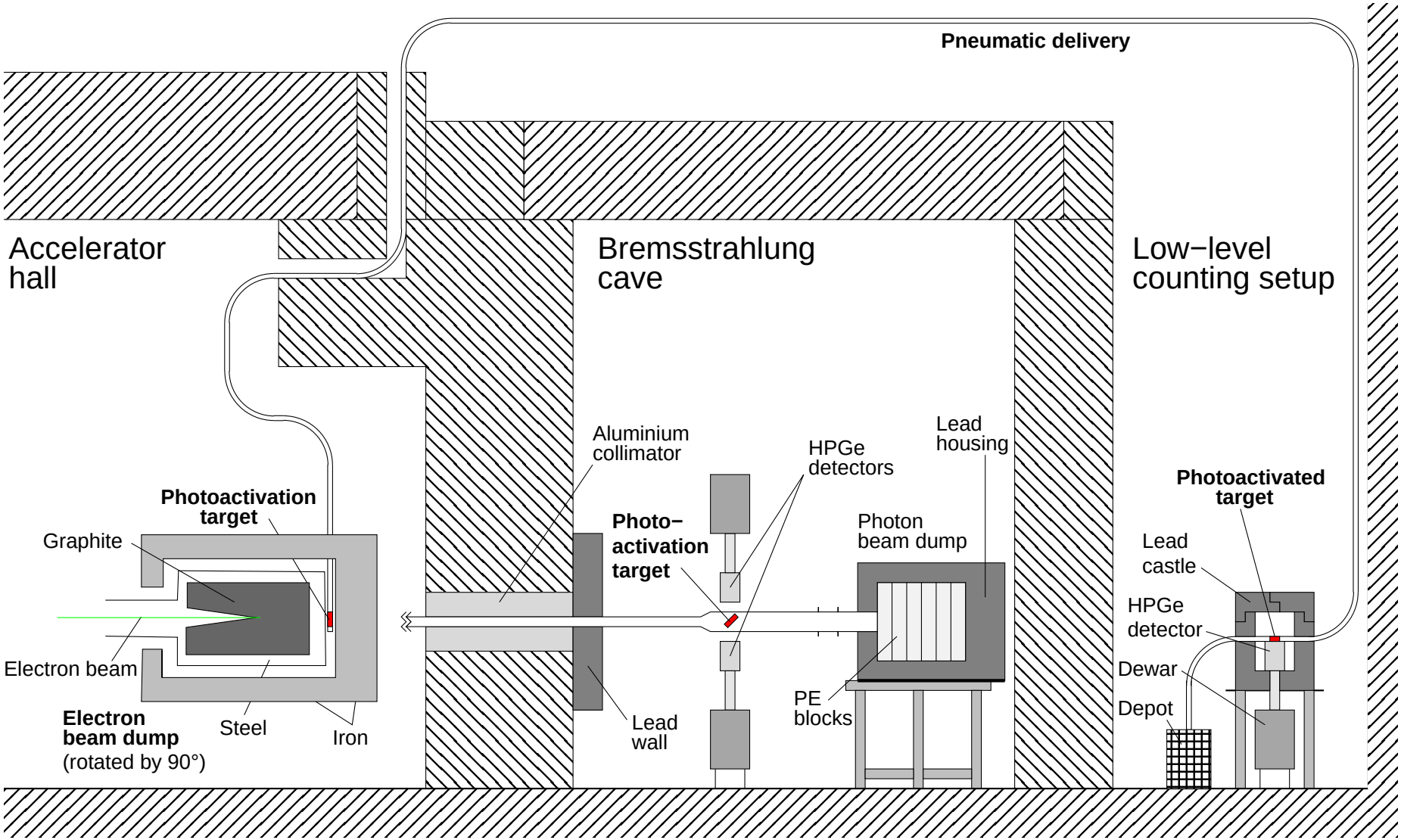

Activation yield

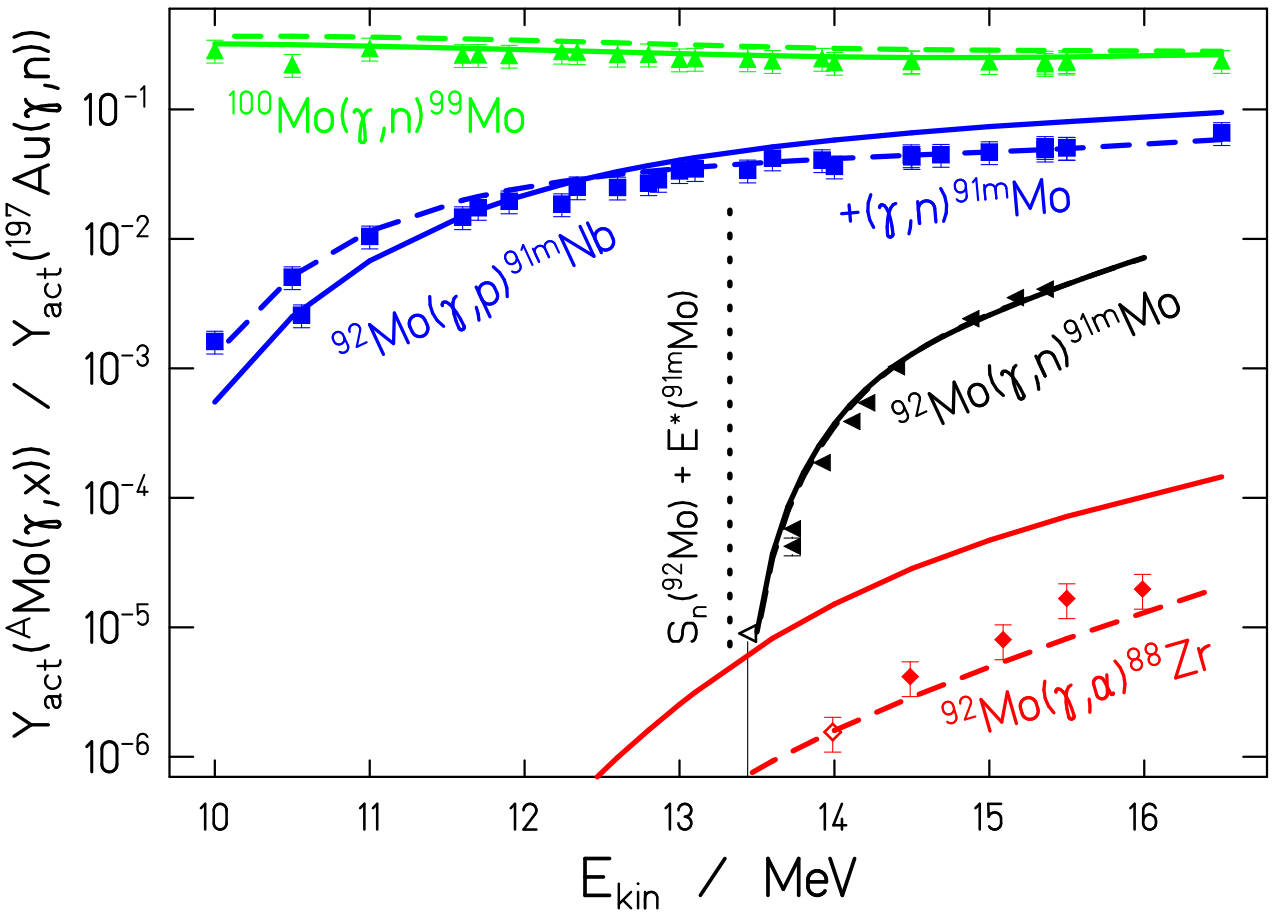

Solid lines: NON-SMOKER,
T. Rauscher and F.-K. Thielemann,
ADNDT 88 (2004) 1

Dashed lines: TALYS,
A. Koning et al.,
AIP Conf. Proc. 769 (2005) 1154

Activation yields of Mo isotopes normalised to the activation yield of the ^{197}Au(γ, n) reaction.

Activation yield

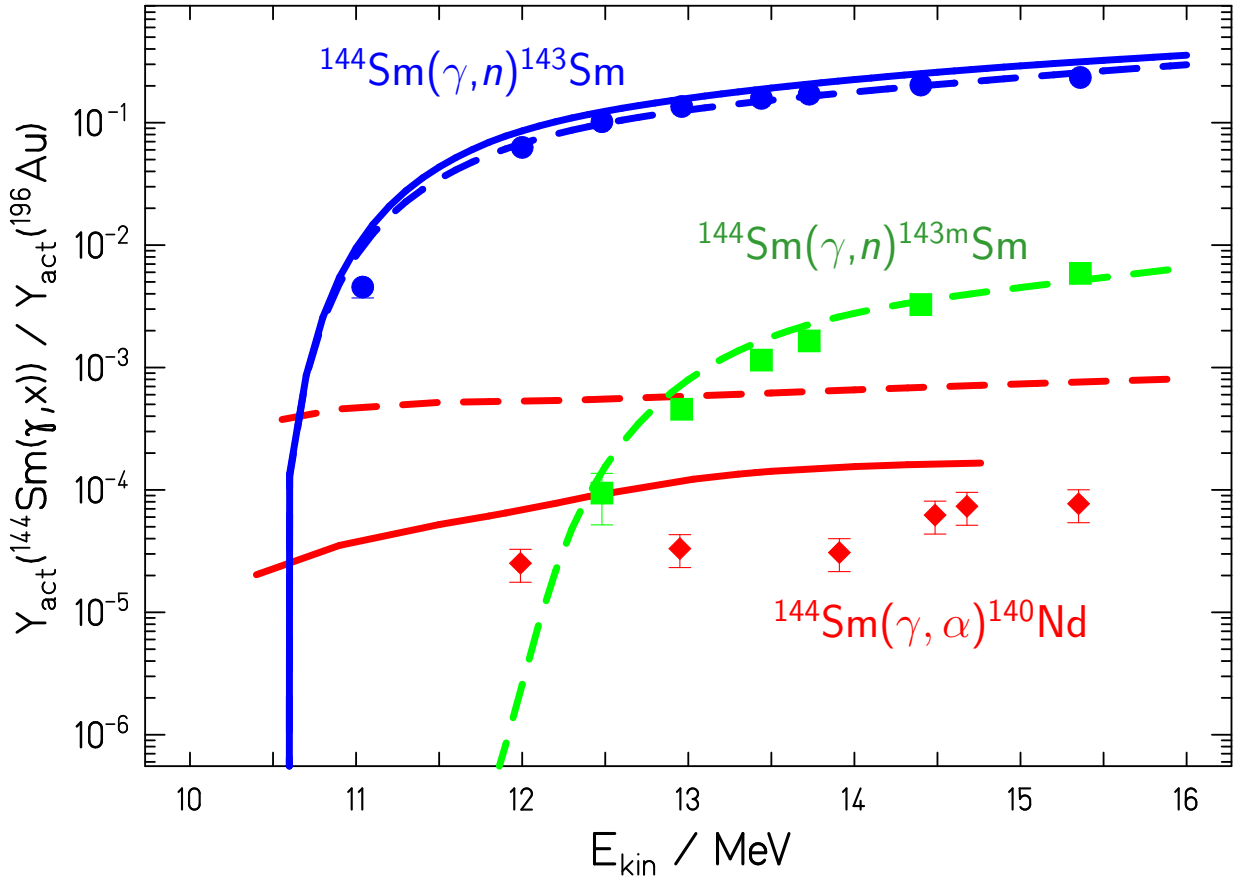

Solid lines: NON-SMOKER,
T. Rauscher and F.-K. Thielemann,
ADNDT 88 (2004) 1

Dashed lines: TALYS,
A. Koning et al.,
AIP Conf. Proc. 769 (2005) 1154

Activation yields of ^{144}Sm normalised to the activation yield of the ^{197}Au(γ, n) reaction.

Activation yield – low-background measurement

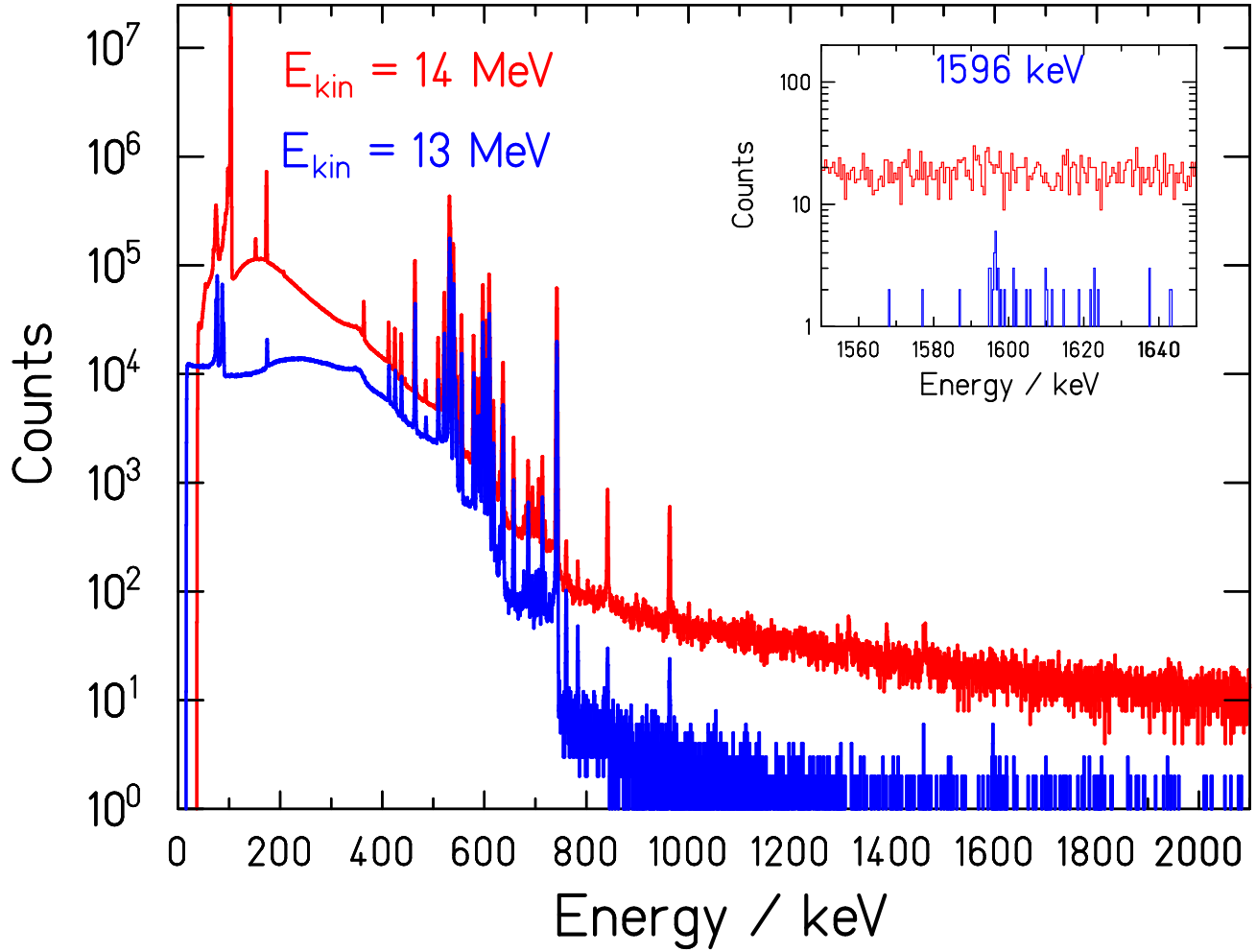

Spectra of the decay of $^{140}Nd \rightarrow {}^{140}Pr \rightarrow {}^{140}Ce$ following the $^{144}Sm(\gamma, \alpha)$ reaction.

Measured in ELBE building

Measured in underground lab "Felsenkeller" in Dresden

Summary

- Photodissociation of Mo isotopes and of ^{144}Sm studied via photoactivation at the ELBE accelerator.
- Determination of the photon flux in the electron-beam dump by means of the ^{197}Au(γ, n) reaction.
- Measurement of weak decay rates in an underground lab.
- ^{92}Mo$(\gamma, \alpha)^{88}$Zr and ^{144}Sm$(\gamma, \alpha)^{140}$Nd reactions observed for the first time at astrophysically relevant energies.
- Rough agreement with predictions of Hauser-Feshbach models for (γ, n) and (γ, p) reactions. Predictions differ for (γ, α) reactions.